Supplementary Materials for

^{18}F-positron-emitting/fluorescent labeled erythrocytes allow imaging of internal hemorrhage in a murine intracranial hemorrhage model

Ye Wang[1], Fei fei An[1], Mark Chan[1], Beth Friedman[2], Erik A. Rodriguez[2], Roger Y. Tsien[2,3], Omer Aras[4*], and Richard Ting[1*]

[1] Molecular Imaging Innovations Institute (MI3), Department of Radiology, Weill Cornell Medical College, New York, NY 10065, USA.

[2] Department of Pharmacology, University of California, San Diego, La Jolla, CA 92093, USA.

[3] Howard Hughes Medical Institute, La Jolla, CA 92093, USA.

[4] Department of Radiology, Memorial Sloan Kettering Cancer Center, New York, NY, 10065

Corresponding Authors: Richard Ting, Molecular Imaging Innovations Institute (MI3), Department of Radiology, Weill Cornell Medical College, 413 East 69th Street. New York, NY 10065, USA, E-mail: rct2001@med.cornell.edu or Omer Aras, Department of Radiology, Memorial Sloan Kettering Cancer Center, New York, NY, 10065, E-mail: araso@mskcc.org

TEL: 6469626195 FAX: 6469620577

Table of Contents

Additional Attached Supplementary Materials

Movie S1. PET-only projection of Figure 3Ai demonstrating the utility of [^{18}F]-RBC-1 in visualizing cryolesion-induced hemorrhage.

Movie S2. PET-only projection of control Figure 3Bi showing no [^{18}F]-RBC-1 signal in the brain of a mouse that does not bear hemorrhage.

Movie S3. Brightfield, PET(red)/CT(blue) projection of figure 4A, the ex vivo brain of Figure 3Ai, and Supporting video 1 mouse, demonstrating a clear co-registration of [^{18}F]-RBC-1 signal with ex vivo bright-field hemorrhage.

Movie S4. Video of Supporting Figure 12. PET(red)/CT(blue) rotation of brain and bright field imaging showing hemorrhage correlating with PET signal 5.3 hours post injection.

Supporting Figure 1. Expanded image of figure 2

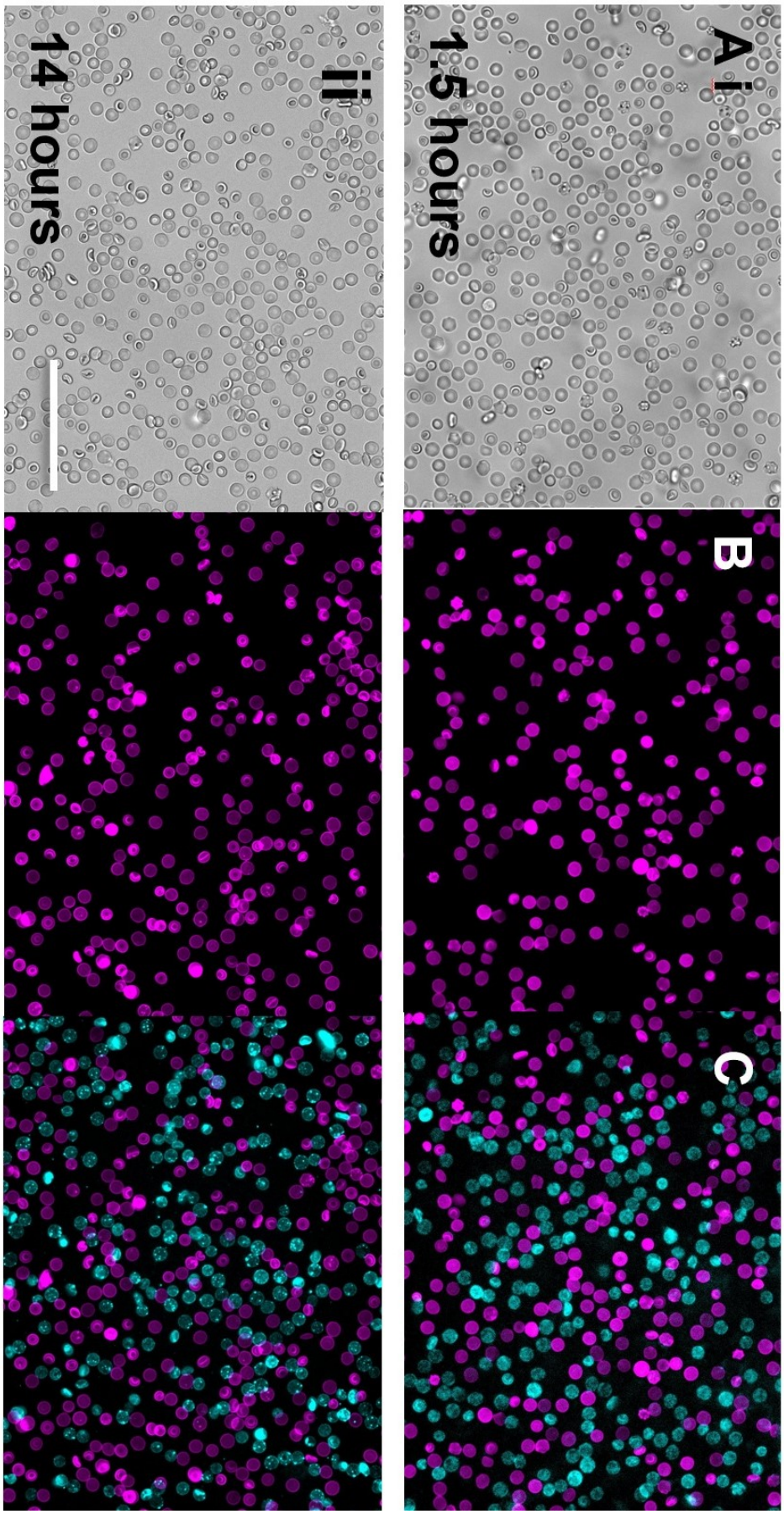

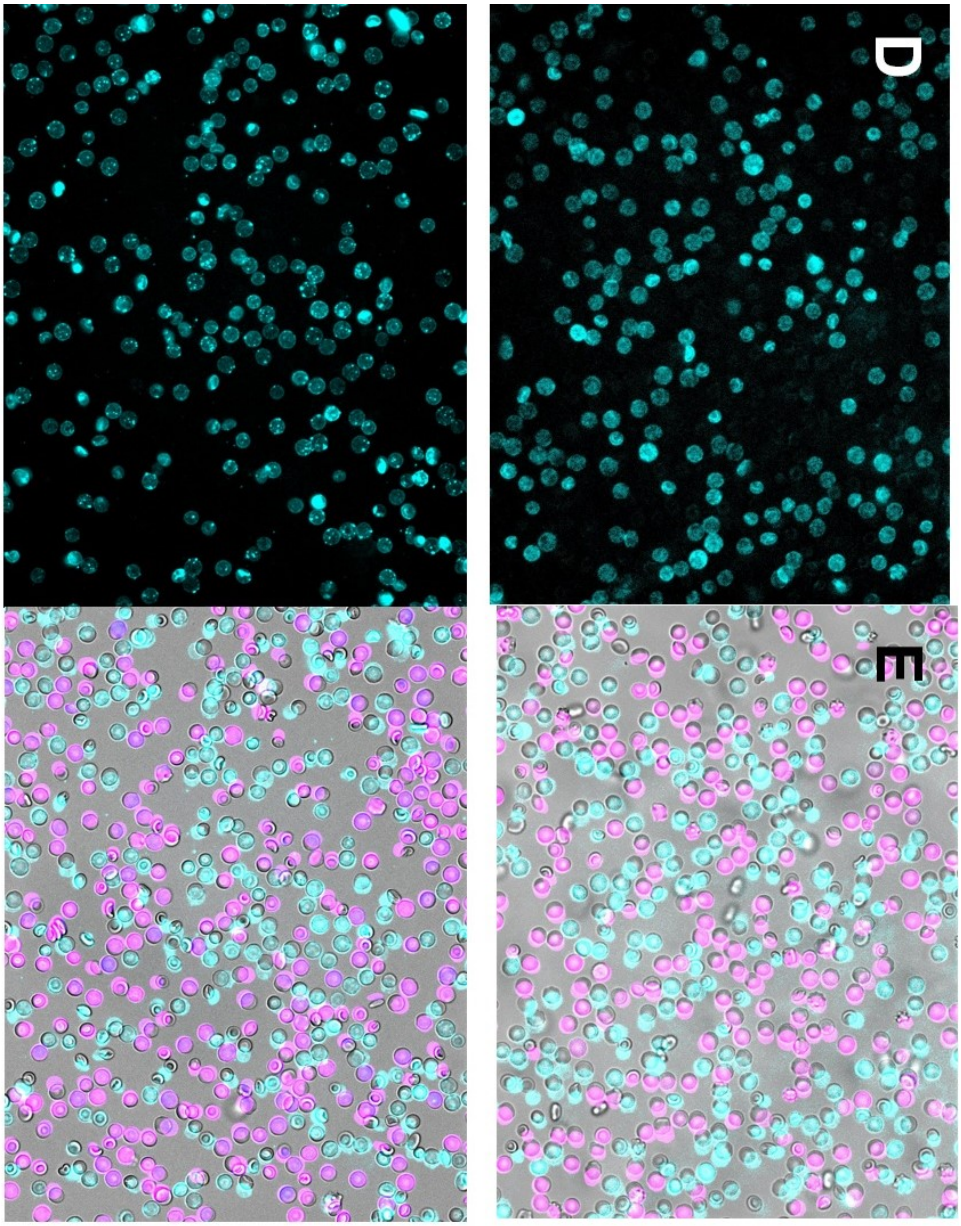

Supporting Figure 1. Expanded image of figure 2. In a mixture of [^{18}F]-PET/NIRF RBCs cells labeled with **1** (Cy3, magenta) and **2** (Cy5, cyan) the fluorescent label remains bound to the original RBC to which it was introduced and does not transfer to other cells even after 14 hours, as shown by the absence of observable cells in two fluorescence channels. RBCs labeled with compound **1** were mixed with RBCs that were labeled with compound **2** and are left at 25 ˚C for 14 hours. (**A**) Unfixed bright field imaging of mixed **RBC-1** and **RBC-2** cells. (**B**) **RBC-1** imaged under fluorescent conditions using 531(40) nm excitation and 593(40) nm emission filters. (**C**) An overlay of fluorescent RBC-1 and RBC-2 show that there was no mixing of **1** or **2** on RBCs after 14 hours. (**D**) RBC-2 imaged using 628(40) nm excitation and 692(40) nm emission filters. (**E**) An overlay of bright field and fluorescent images (**A, C**) show that RBCs contained the original dye that they were labeled with, and that 1 or 2 were evenly distributed to RBCs. Scale bar: 50 μm. Top series (**i**): imaging 1 hour after mixing. Bottom series (**ii**): imaging 14 hours after mixing.

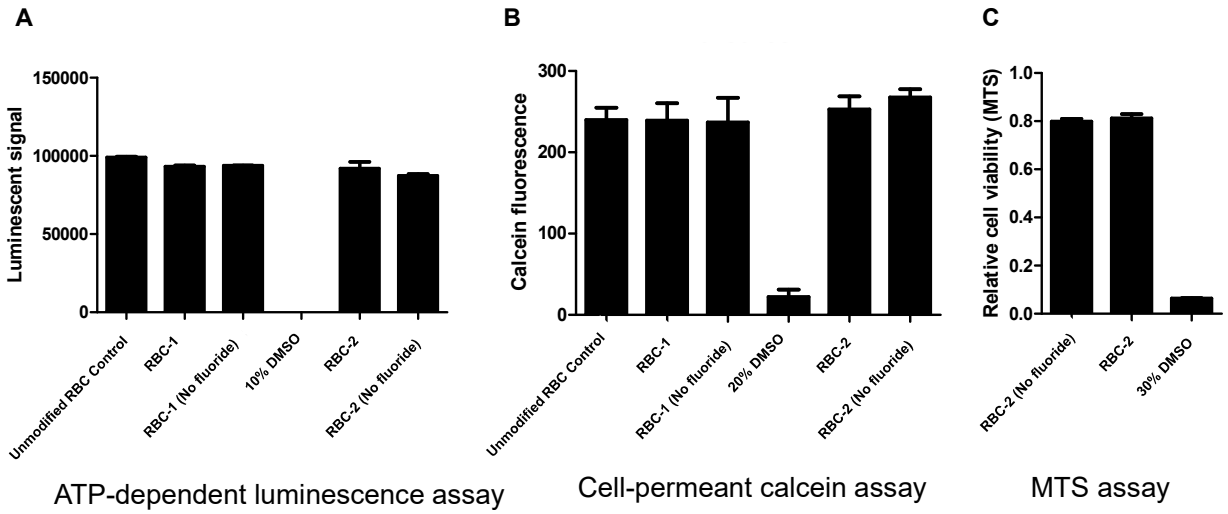

Supporting Figure 2. Confirmation of RBC viability following the labeling of RBCs with [18F]-PET/NIRF probes 1 (Cy3) and 2 (Cy5). RBCs labeled with compound **1** and **2** were assayed for cell viability using commercial kits including: (**A**) a luminescent ATP detection assay, a (**B**) cell-permeant calcein assay, and (**C**) a cell proliferation assay. Controls included unmodified RBCs (positive control) and non-viable RBCs that had been inactivated with DMSO (negative control). Blood (500 µL) was collected from an anesthetized BALB/C mouse by cardiac puncture in the presence of heparin as an anti-coagulant. Isolated RBCs were re-suspended with 10 ml PBS, and washed 3 times with 10 ml PBS in a centrifuge at 200 rcf for 20 minutes. 1 mL aliquots of blood were distributed to six vials: Vial 1 contained 1 mL of unmodified RBCs ($1.5x10^8$ cells, positive control); Vials 2 and 4 contain 1 mL of blood and 2.5 µL of **1** or **2** which were pre-reacted with 2.5 µL of 200 mM HF for 1 hour, and neutralized with 5 µL of 10 x PBS, to give **RBC-1** and **RBC-2**; Vials 2 and 4 contain 1 mL of blood added to 2.5 µL of **1** and **2** that were not treated with fluoride. Vial 6 contained 1 mL of blood and 111 µL of DMSO (negative control). The mixtures were incubated for 30 minutes. Labeled cells were then washed with RPMI-1640, 10% FBS media, 3 times in a centrifuge set at 200 rcf for 20 minutes. All vials were re-suspended in 10 mL of medium and seeded into each well of a 96-well plate with black walls and clear bottoms (100 µL/well). An ATP-dependent luminescent cell viability assay, cell-permeant calcein AM assay, and an MTS cell proliferation assay were used to verify RBC viability on a Tecan Infinite M1000. The ATP-dependent luminescence assay was performed with the addition of 100 µL CellTiter Glo reagent (Promega, Cat# G7572) into each well followed by incubation at room temperature for 15 minutes. Luminescence settings were used to collect data. For the Calcein AM assay, 100 µL of 4 µM Calcein AM (Biotium, 30026) in PBS was added into each well. The mixture was incubated at 37˚C for 30 minutes. Fluorescence was measured with an excitation wavelength of 485 and emission filter at 530 nm. For the MTS cell proliferation assay, 20 µL of CellTiter 96 Aqueous One reagent (Promega, Cat# G358C) was added into each well. The mixture was incubated at 37˚C for 4 hours. Absorbance was measured at 490 nm.

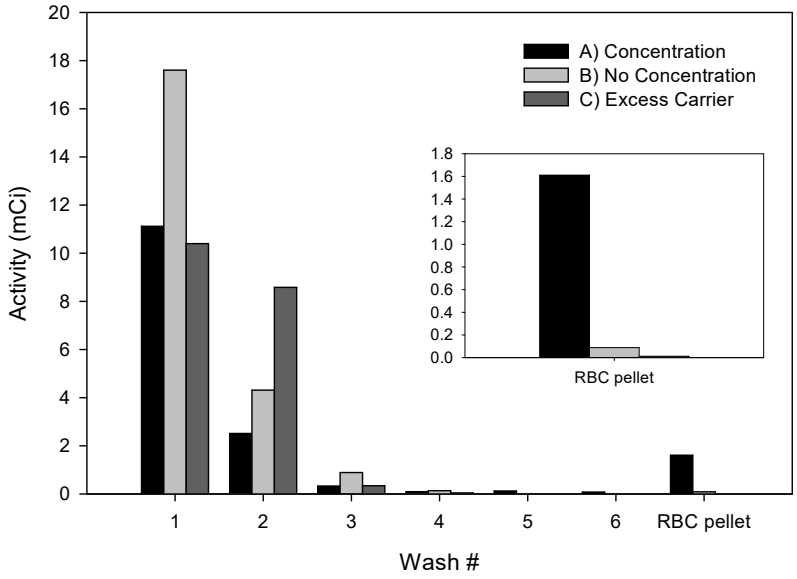

Supporting Figure 3. Radiochemical analysis of [18F]-RBC purification by centrifugation. Six washes of RBC (with 15 mL of PBS) were performed to remove unreacted, NHS-ester **1**, [^{18}F]-fluoride ion, and hydrolyzed **1** or **2**, away from [^{18}F]- RBC. Three different labeling conditions were performed/attempted on RBC. (**A**) NHS containing **1** was labeled with 60 mCi of [^{18}F]-fluoride ion in a 1 to 4 ratio of **1** to fluoride. Concentration of the mixture was performed before neutralization, RBC addition, and PBS washes (6). The resulting [18F]-RBC activity obtained was 1.6 mCi after 6 PBS washes. (**B**) To confirm that RBCs do not take up fluoride non-specifically, NHS-**1** was labeled with 71 mCi of [^{18}F]-fluoride ion in a 1 to 3 ratio of **1** to fluoride. Concentration of this mixture to a fluoride concentration that is greater than 20 mM was NOT performed before neutralization and RBC addition. The resulting [18F]-RBC activity obtained was 4 μCi, 400 fold less (3.5 hour synthesis, decay uncorrected), and could not be imaged in brain in or ex vivo (**C**) The labeling of **1** was performed a third time, with 46 mCi of [^{18}F]-fluoride ion, in the presence of a large excess of ^{19}F carrier fluoride in a 1 to 125 ratio of **1** to fluoride. Concentration of the mixture was performed before neutralization, RBC addition, and PBS wash (6). The resulting [18F]-RBC activity obtained was <1 μCi. Only condition **(A)** resulted in the desired, labeled **[^{18}F]-RBC**.

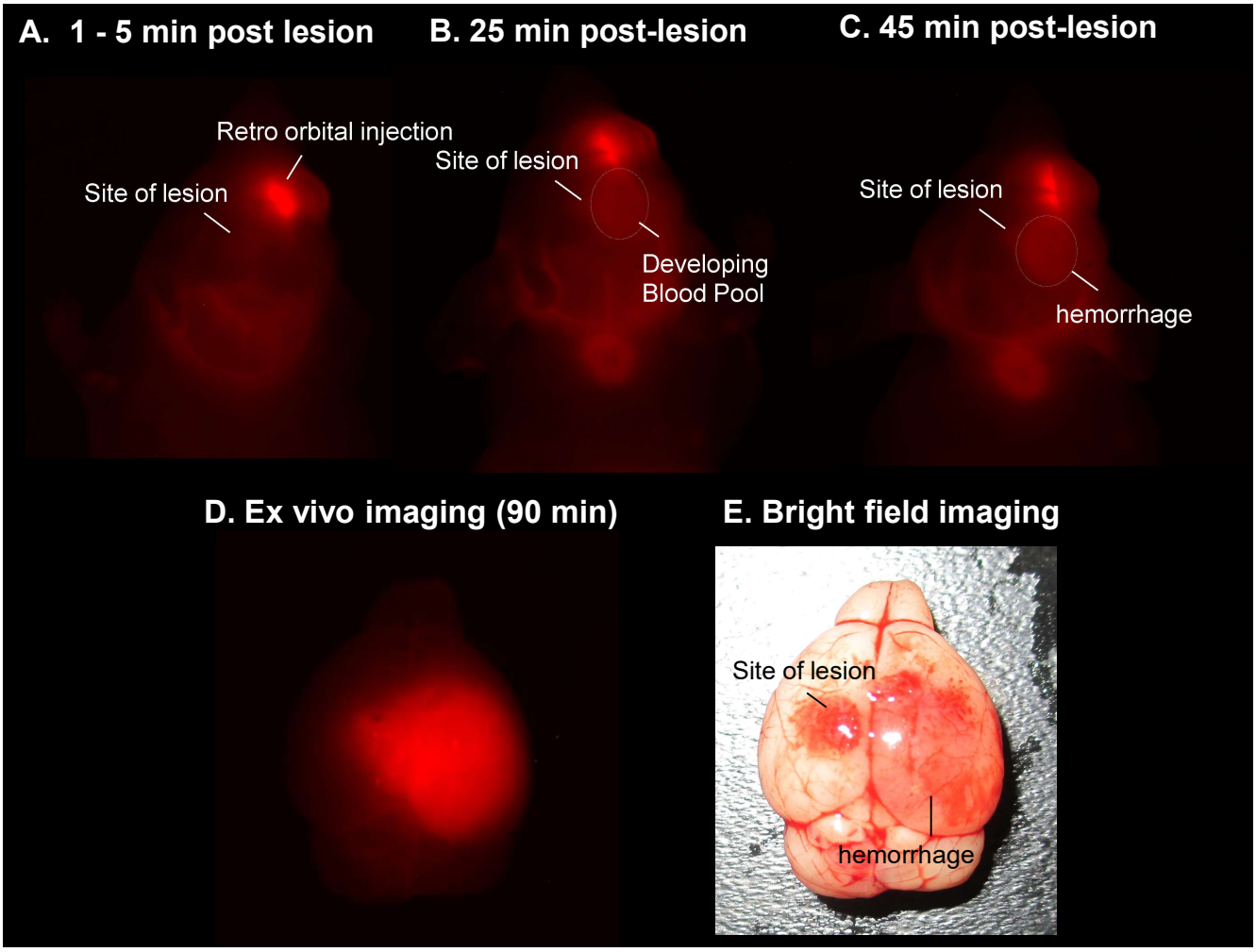

Supporting Figure 4. Fluorescence from [^{18}F]-PET/NIRF 2 could be used to image hemorrhage in vivo. Near infrared imaging of agent labeled with Cy5 dye **2**. Real time observation of traumatic progression: (**A**) 1 to 5 min post-lesion, (**B**) 25 min post-lesion, and (**C**) 45 min post-lesion in a skull-exposed cryolesion bearing mouse. Note the growing blood pool. (**D**) ex vivo fluorescence imaging showing blood pool in the brain. Imaging is clearer than (**A-C**) due to removal of skull (**E**) bright-field imaging confirming site of lesion and hemorrhage.

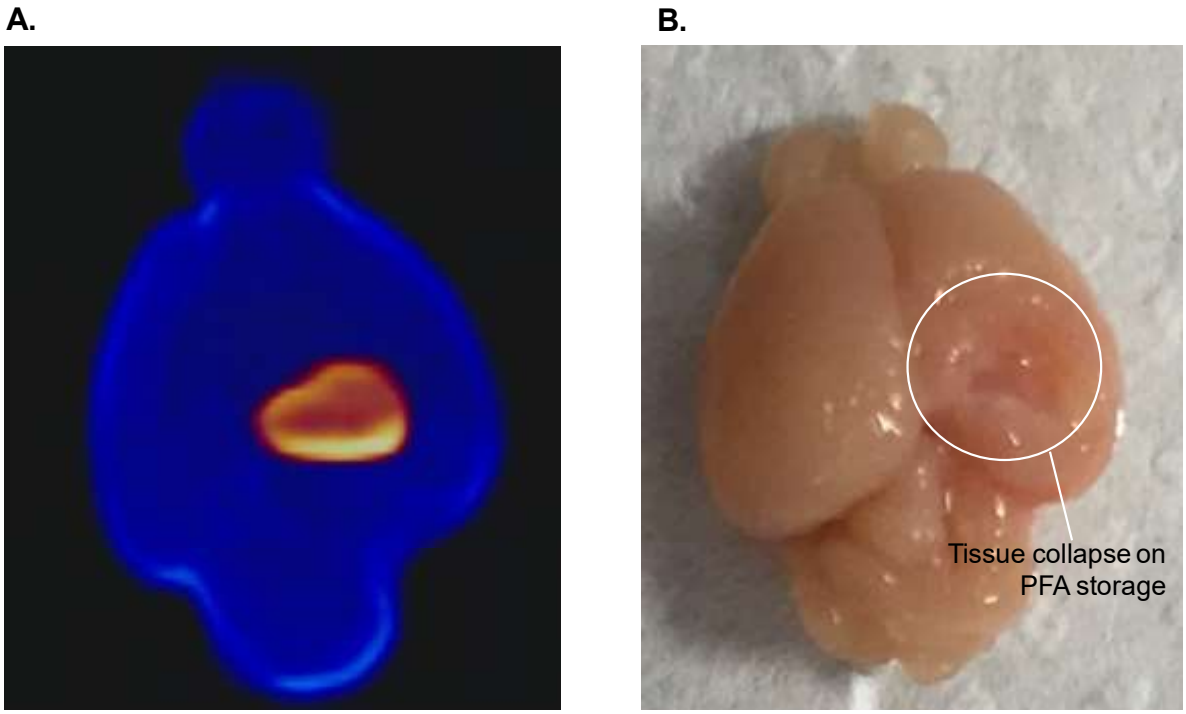

Supporting Figure 5. ex vivo RBC-1 [18F]-PET imaging of intracranial hemorrhage. (**A**) ex vivo PET/CT brain image of a tail vein injection of **RBC-1** of a mouse 40 min after cryolesion. In an attempt to preserve brain tissue for PET/MR imaging, brain tissue was preserved in 4 °C, refrigerated 4% paraformaldehyde PBS solution for a week following PET acquisition. (**B**) *Ex vivo* bright field imaging after week long PFA storage clearly showed a lesion corroborating the **[**^{18}F**]-RBC-1** signal in the PET/CT; however, macroscopic coloration corresponding to the presence of viable RBCs at the site of lesion was not present. Additionally, the region of brain tissue containing the hemorrhage had clearly disintegrated. An MR of this tissue did not provide any more meaningful data than the bright field image. For three dimensional co-registration of PET and MR hemorrhage data, imaging must be performed on fresh tissue.

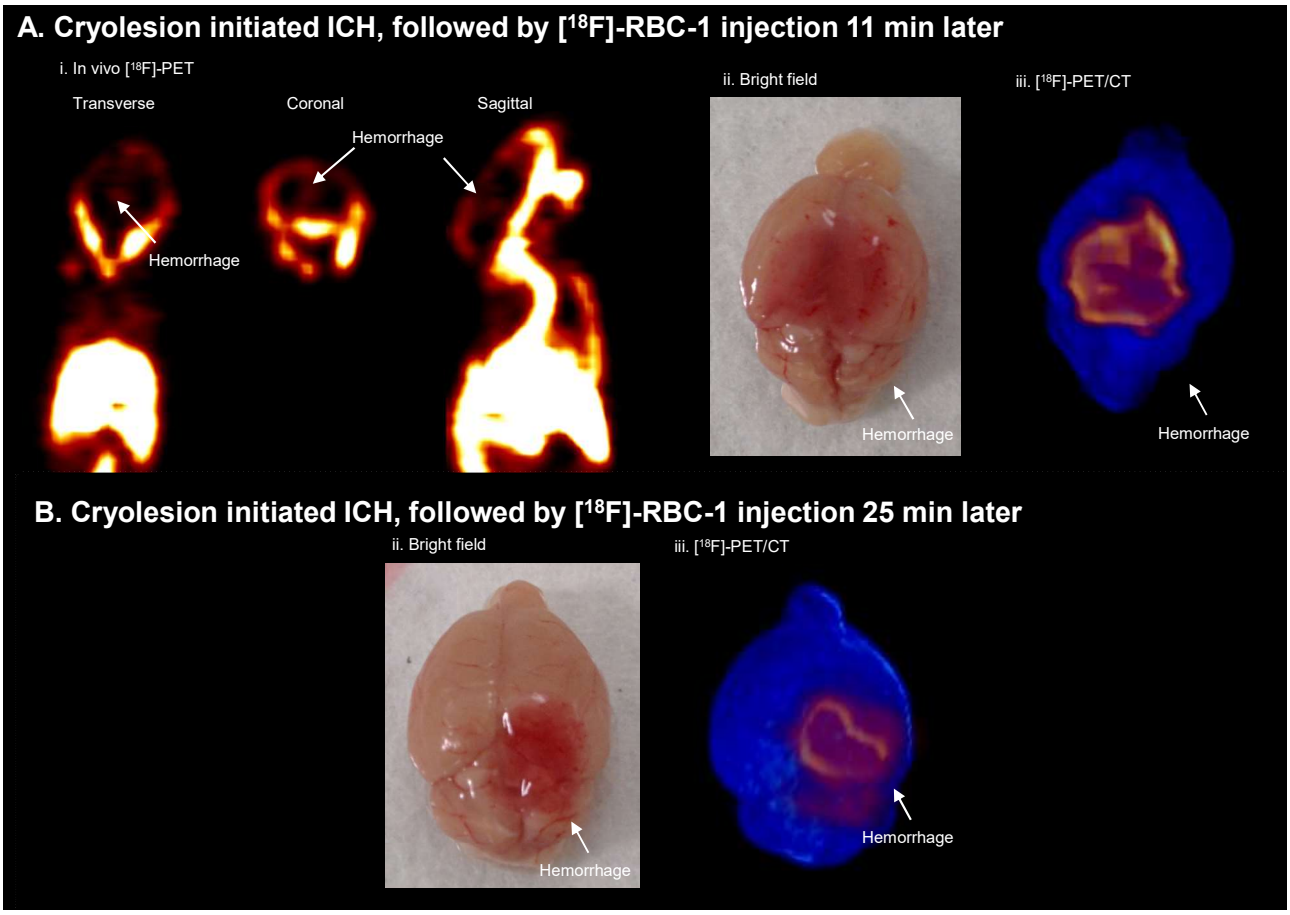

Supporting figure 6. Intracranial hemorrhage was observed in and ex vivo, after temporal delays were inserted between cryolesion and [^{18}F]-RBC-1 injection. **[^{18}F]-RBC-1** is used to image intracranial hemorrhage following a delay between cryolesion and **[^{18}F]-RBC-1** injection. Cryolesions were initiated in mice under isofluorane anaesthesia. Time was allowed to pass before **[^{18}F]-RBC-1** was introduced through the tail vein. (**Ai**) Transverse, coronal, and sagittal PET slices of a mouse that had received a cryolesion 11 min before **[^{18}F]-RBC-1** was introduced through the tail vein. Intracranial hemorrhage was indicated in each slice with white arrows. Intracranial hemorrhage is confirmed by bright field (**ii**) and PET/CT (**iii**) imaging of this brain following immediate excision after whole body image acquisition. (**B**) Bright field (**ii**) and PET/CT (**iii**) imaging was used to confirm intracranial hemorrhage after a 25 min delay was inserted between cryolesion and **[^{18}F]-RBC-1** tail vein injection.

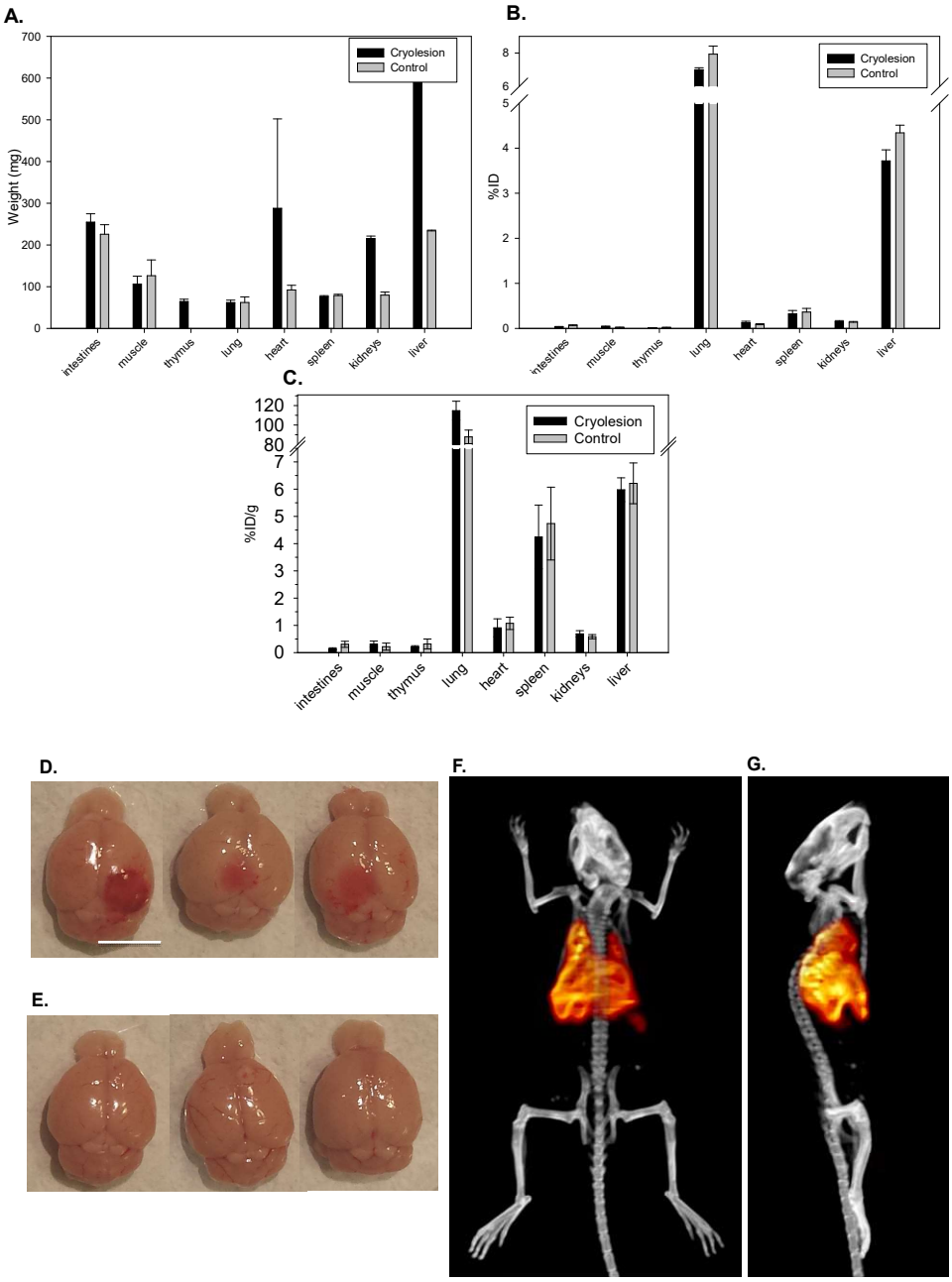

Supporting Figure 7. Scintillated biodistribution of [^{18}F]-RBC-1 60 min after cryolesion and tail vein injection. (**A**) The general biodistribution of **RBC-1** after 50 min following tail vein injection is to lung, spleen, and liver. There was minimal localization of **RBC-1** to intestines, kidneys, and muscle, suggesting that **RBC-1** can be used to visualize other bleeding disorders such as intestinal bleeding, renal bleeding, and more general internal bleeding in emergency situations. Tissue weight obtained 1 hour after **RBC-1** injection and cryolesion (n = 3 mice with cryolesions and n = 3 control mice with no cryolesion), error bars = SEM. (**B**) [^{18}F]-scintillated bio distribution reported in percent injected dose (%ID) and **(C)** percent injected dose per gram (%ID/g). Note that brain hemorrhage did not significantly affect distribution of RBC-1 in other tissues Error bars = SEM. Fresh blood for biodistribution was collected from the left ventricle of a functional heart immediately following cervical dislocation. (**D**) *Ex vivo* bright-field imaging of brains bearing intracranial hemorrhage in cryolesion cohort.

(**E**) Images of brains of mice in control cohort. Note that brain hemorrhage did not significantly affect distribution of **RBC-1** in other tissues. Scale bar: 0.5 cm. (**F**) Ventral and (**G**) side PET/CT projections confirming distribution data in (**B** & **C**). Images were contrasted to focus on the major organs of **RBC-1** distribution in mice. Note the general lack of **RBC-1** in the abdominal regions of mice suggesting that [^{18}F]-RBCs should be additionally useful in the imaging of intestinal bleeding, renal bleeding, and internal bleeding in emergency situations.

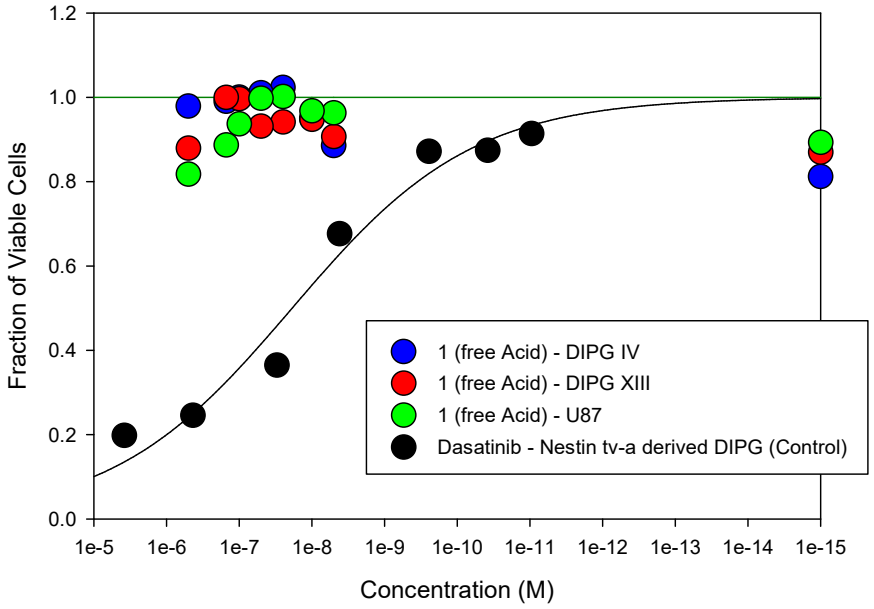

Supporting figure 8. [^{18}F]-RBC-1 does not trigger glial toxicity. Cell viability studies were carried out as described in Supporting figure 2. High-concentration solutions of **1** were incubated with different immortal glial cell lines. Toxicity was not observed when high concentrations of **1** were incubated with for 48 hours or more with DIPG IV, DIPG XIII, or U87 cell lines. A reference consisting of dasatinib (Sprycel, Bristol Myers Squibb) in Nestin tv-a derived DIPG is shown as a control IC_{50} 19 ± 20 nM, R^2 = 0.972 four parameter logistic standard curve regression analysis. Toxicity due to **1** is not observed.

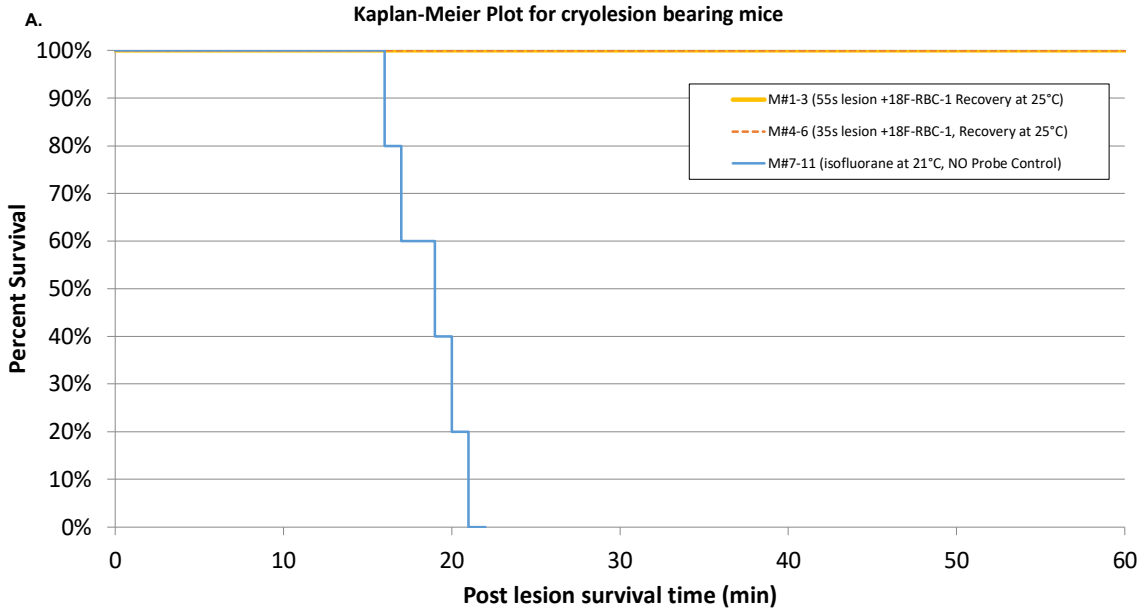

Supporting figure 9. Kaplan-Meier Plot showing that cryolesion/PET associated hypothermia can be avoided with recovery between cryolesion and scanning. Mortality due to cryolesion-related hypothermia can occur in the bore of an Inveon PET/CT calibrated at 21 °C. A warmed recovery step must be implemented between cryolesion and imaging to avoid mortality (M#1-3, M#4-6, orange and yellow lines). If mice are immediately transferred from the operating table to the bore of an Inveon PET/CT (calibrated at 21 °C) following cryolesion, death can occur (M#7-11, blue line). The following experiment identifies hypothermic death due to cryolesion (and not toxicity of **1**) if cryolesion is directly proceeded by PET/CT imaging, without a recovery step. Note that morbidity can also be reduced by reducing cryoprobe contact time.

Three cohorts of mice were prepared. Cohort A, consisting of 3 mice (M# 1, 2, 3) were anesthetized with isoflurane and exposed to a cryoprobe for 55s (100 g of pressure, 7.9 g/mm^2, over a 12.6 mm^2 contact area). Mice in Cohort B (3 mice, M# 4, 5, 6) were anesthetized and exposed to shorter, 35s, cryolesion contact times focused on the right posterior cerebral cortex. Immediately following cryolesion, these 6 mice (Cohort A and B) were injected with **[^{18}F]-RBC-1** (tail vein), disconnected from isoflurane anesthesia, and were immediately transferred to a cage heated to 25 °C using a temperature-controlled space heater, where all 6 mice were allowed to recover. All 6 mice survive to the point of deliberate sacrifice, for longer than 3 hours at 25 °C. Photography taken between 1-3 hours show viable, cryolesion bearing mice (not shown, available upon request). A control cohort, Cohort C, consisting of 5 mice, were anesthetized and were treated with 55s cryolesions focused on the right posterior cerebral cortex. This cohort, **Cohort C, WAS NOT injected with any agent**, i.e. these mice receive cryolesion but no PET injectate (NO-probe control). Following cryolesion, Cohort C mice are maintained under isoflurane and immediately transferred into the bore of an Inveon PET/CT that is calibrated at 21 °C. Kaplan-Meier plot (shown above) demonstrate that all post-cryolesion mice in cohort C die between 15 and 25 min in the bore of the PET scanner. Mortality from cryolesion-PET/CT imaging is due to cryolesion-related hypothermia. Mortality is not related to the injected **[^{18}F]-RBC-1** imaging agent. Mortality can be eliminated by allowing mice to recover in a warmed cage immediately following cryolesion. Mice receiving cryolesions with a reduced contact time (Cohort B, 35s) showed smaller volume lesions in

PET/CT analyses vs. Cohort C, where cryoprobe contact time is longer (55s) (compare bright-field and PET data in supporting figure 13f,g (PET/CT of M# 4 and 6 brain) to supporting figure 11 and 13h-l).

Supporting figure 10. Additional histology of cryolesion/intracranial hemorrhage bearing brains (stored as frozen -78 °C, PBS buffered optimal cutting temperature blocks).

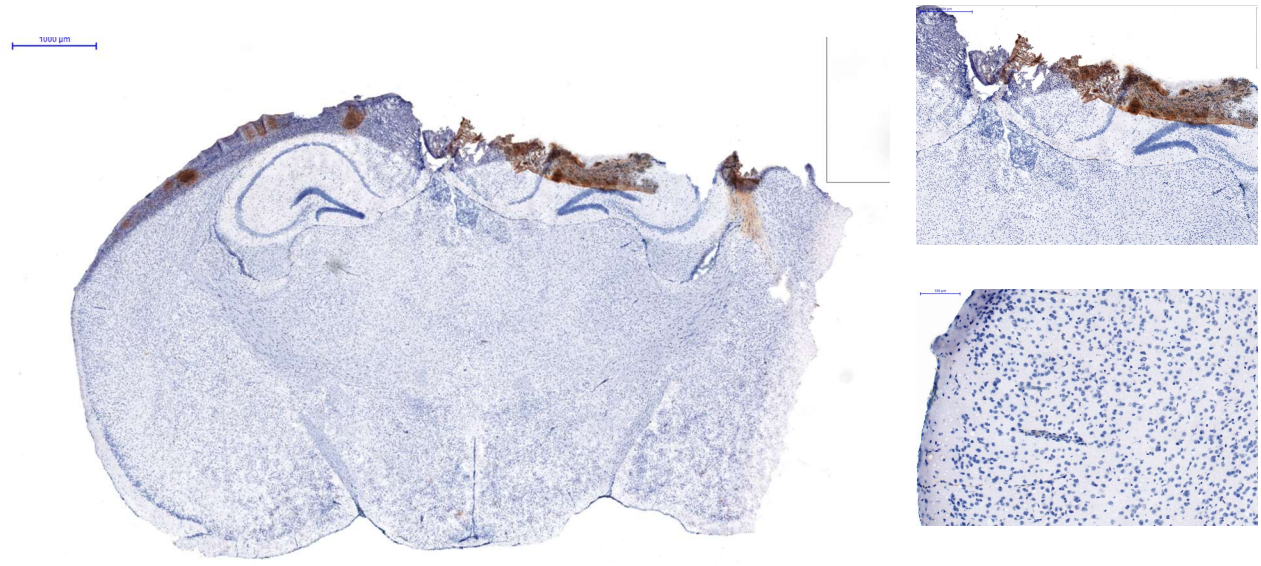

i. Specimen from Supporting Figure 11A, and 13H

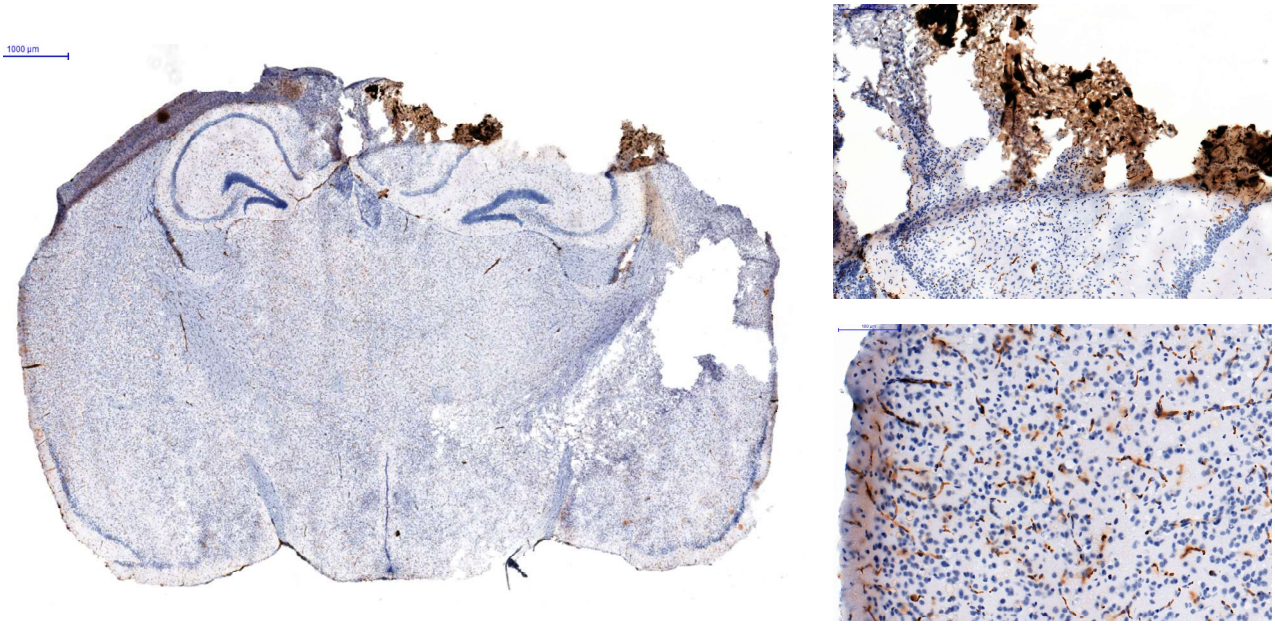

ii. Specimen from Supporting Figure 9A, (Cohort B, M4), and 13J

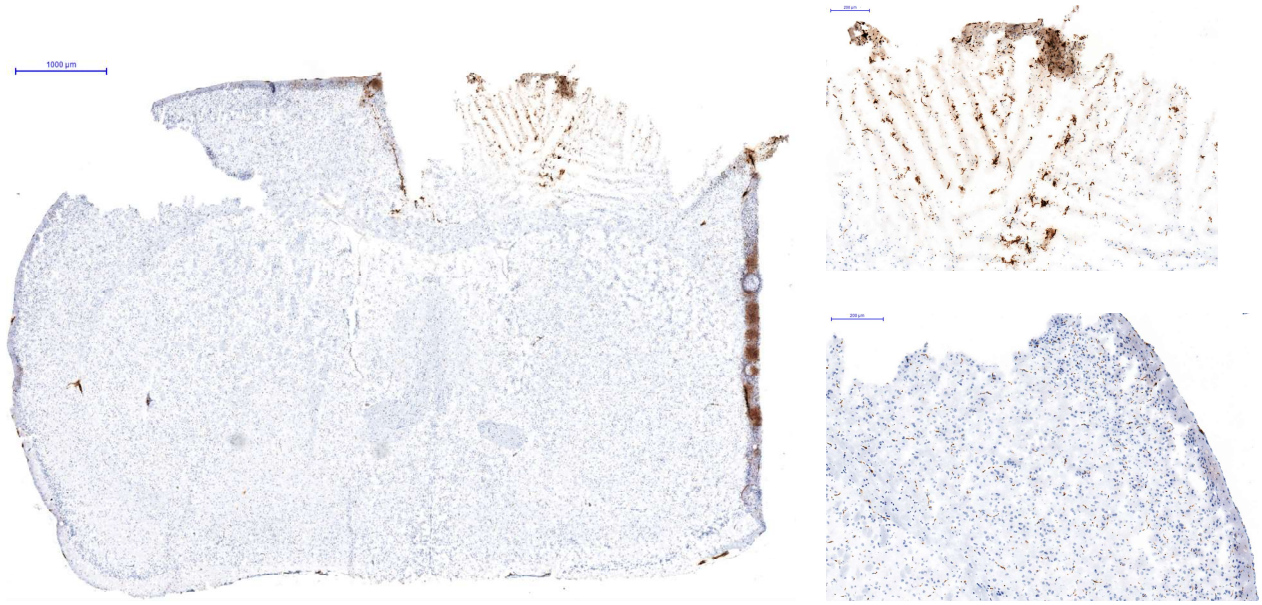

iii. Specimen from Supporting Figure 11B, and 13I

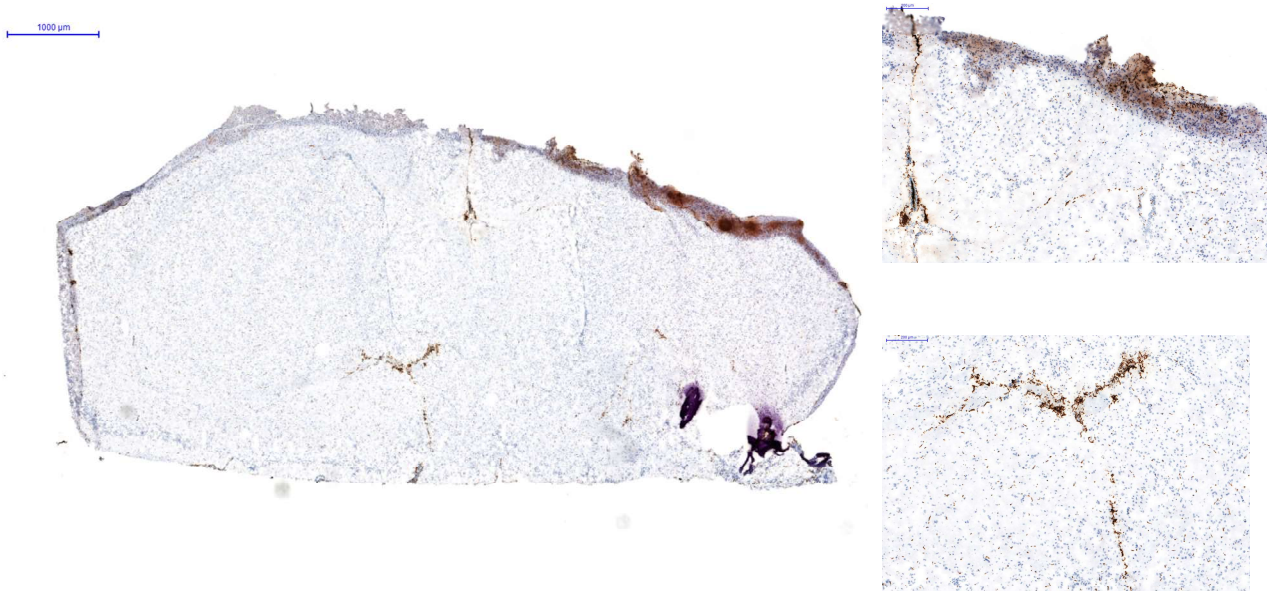

iv. Specimen from Supporting Figure 9A, (Cohort B, M6), and 13g

Presented sections are generated from frozen (-78°C) OCT blocks. Tissue preservation is superior to storage in formalin-fixed paraffin sections stored in 4°C paraformaldehyde solution (Figure 4C). Staining is performed with RBC-specific TER-119 antibody (brown), hematoxylin, and eosin.

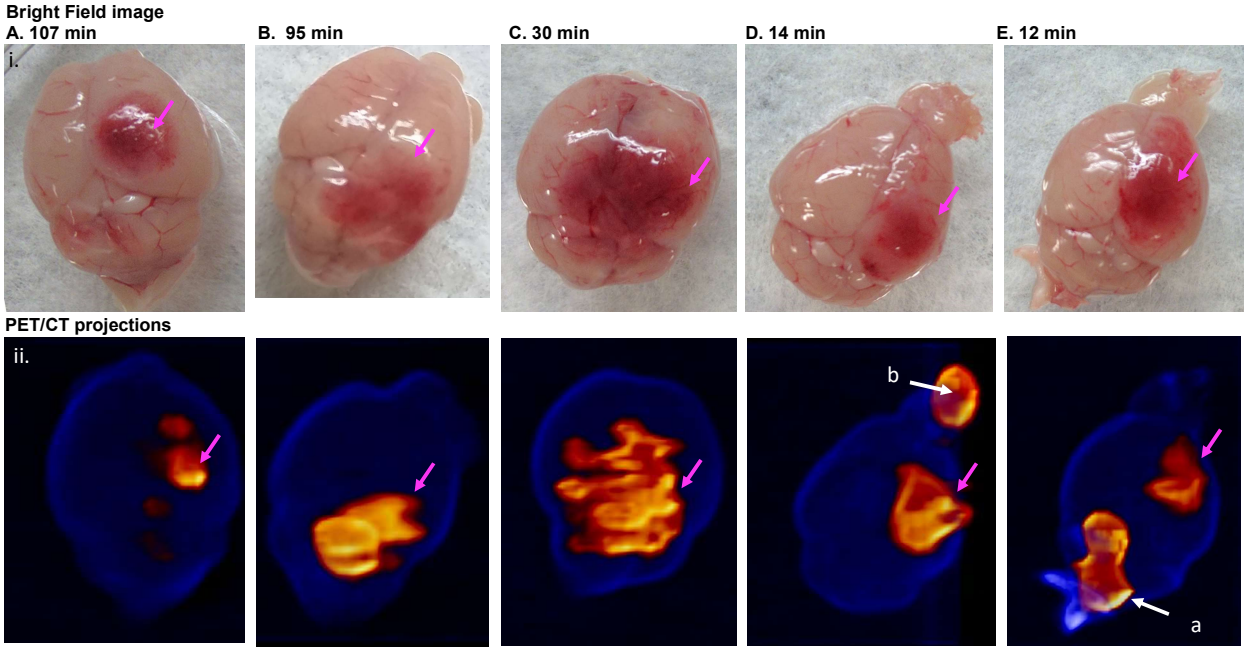

Supporting figure 11. Intracranial hemorrhage can be observed with [18F]-RBC-1-PET 50 to 157 min after cryolesion, after longer temporal delays (12 to 107 min) are inserted between cryolesion and [18F]-RBC-1 injection.

Longer temporal delays were inserted between cryolesion and contrast agent injection (longer delays are used vs. supporting figure 6, where 11 and 25 min delays were implemented). Following cryolesion (55 sec), mice were immediately transferred to a heated cage at 25°C without anesthesia to prevent mortality from hypothermia. The following times were allowed to pass before **[^{18}F]-RBC-1** was introduced through the tail vein: (**A**) 107 min, (**B**) 95 min, (**C**) 30 min, (**D**) 14 min, and (**E**) 12 min. Mice were sacrificed 40 min following injection. Brains were resected and imaged by (**i**) Brightfield and (**ii**) PET (orange)/CT (Blue) imaging.

Artifacts associated with tissue excision are sometimes observed in sectional analyses. E.g. **b**. Bleeding in olfactory bulb that may or may not be related to cryolesion, and **a**. Bone fragment (CT blue) and blood accumulation at the base of the brain possibly from ex vivo drainage following organ excision. Hemorrhage that is visible in bright field and PET/CT is indicated by magenta arrows. Note the significant hematoma accompanying models. (Comprehensive section analysis shown in Supporting Figure 12 h-j)

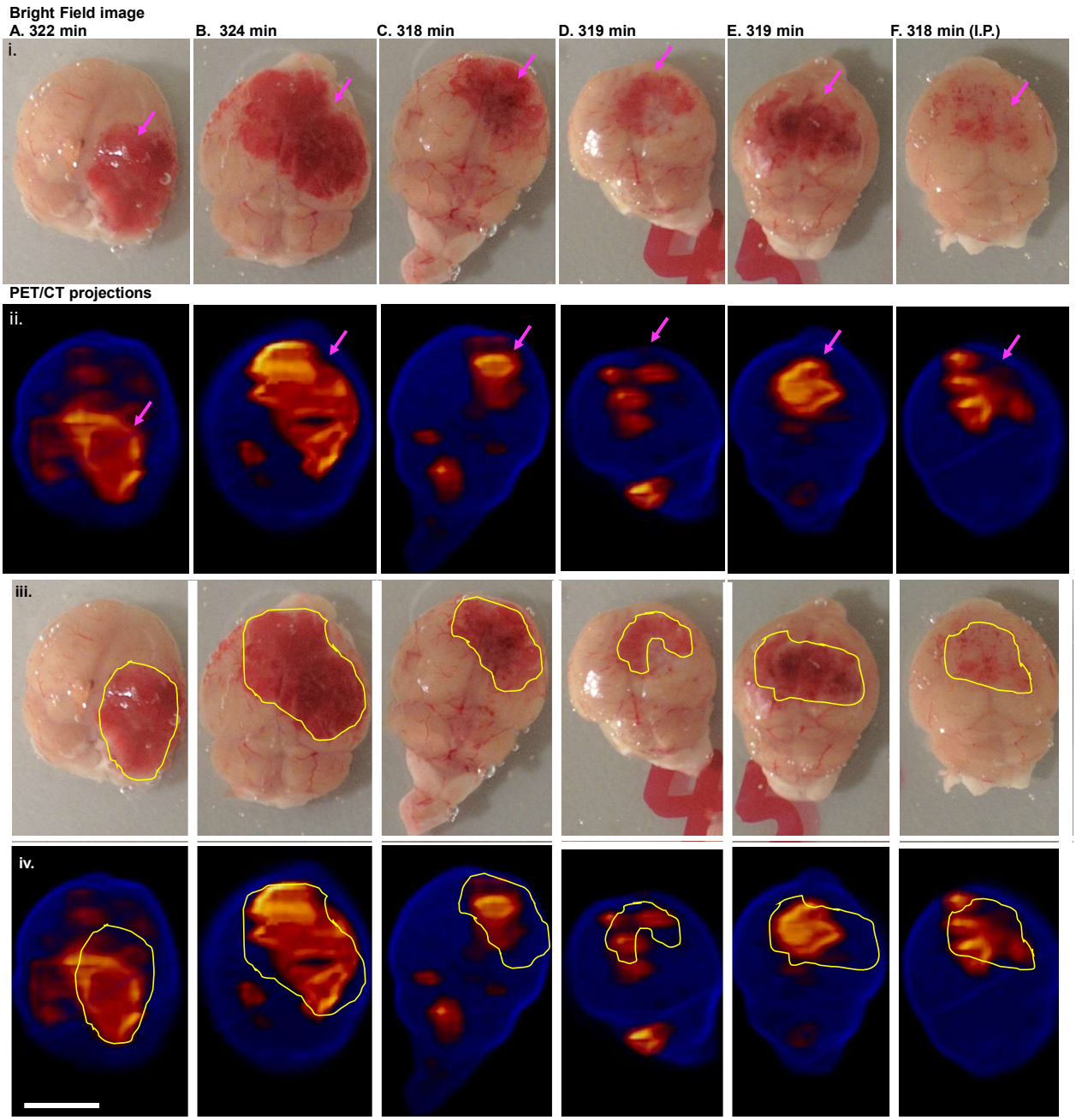

Supporting figure 12. Intracranial hemorrhage can be observed with [18F]-RBC-1-PET 6 hours after cryolesion, following 5.3 hours of delay between cryolesion and [18F]-RBC-1 injection.

Temporal delays of ~5.3 hours were inserted between cryolesion and contrast agent injection. Cryolesion bearing mice (50 sec cryolesion, 100g) were immediately transferred to a heated cage at 25°C without anesthesia to prevent mortality from hypothermia. The following times were allowed to pass before **[^{18}F]-RBC-1** was introduced through the tail vein (i.v.): (**A**) 322 min, (**B**) 324 min, (**C**) 318 min, (**D**) 319 min, and (**E**) 319 min. 90% of **[^{18}F]-RBC-1** was introduced intraperitoneally in (**F**) at 318 min due to failure to

achieve i.v. injection. Mice are deliberately sacrificed, 40 min following injection (~400 min post cryolesion), and brains were resected and imaged by (**i**) Brightfield and (**ii**) PET (orange)/CT (Blue) imaging. All mice survive until the point of sacrifice.

Following long (5.3 h) delay between cryolesion and contrast agent injection, **[^{18}F]-RBC-1** agents distribute to the general region of hemorrhage (millimeter resolution), but do not corroborate brightfield hematoma data (**iii**) exactly, i.e. at the sub-millimeter level. This is expected.

PET/CT data (**iv**) corroborate visible hematoma (delineated in yellow, see (**iii**)) to a **lesser** extent, as **longer** delays are inserted cryolesion and RBC injection (Compare Supporting Figure 12 data with that in Supporting Figures 6 and 11). As a specimen is given time to recover from a hemorrhagic event, local regions which differ in active hemorrhage rates may be generated (from healing, clotting, and progressing hemorrhage). Delayed injections of **[^{18}F]-RBC-1** should be biased to more active regions of bleeding. Scale bar = 0.5 cm. Stand-alone, bright-field hematoma data cannot be used to distinguish between regions of active and inactive/less-active hemorrhage, unlike **[^{18}F]-RBC-1** PET data.

See supporting Movie S4 for tomographic analysis and demonstration/localization of **[^{18}F]-RBC-1** to visible hematoma.

Supporting figure 13. PET/CT sectional analysis of intracranial hemorrhage bearing brain. Analysis of brain samples that bear intracranial hemorrhage are presented. These analyses are to-scale (vs. bright field image) and are comprehensively presented as 1 mm sections (±1 mm) in coronal, sagittal, and horizontal dimensions. PET, CT, and fused PET/CT data is presented. NIH color tables are used to quantitate relative signal. Windowing is not performed (note that accompanying NIH color tables begin at 0.0), i.e. noise is not reduced, and signal to noise is not artificially enhanced. Note that exsanguination/blood vessel perfusion is <u>not</u> performed on brain tissue prior to excision and imaging. Perfusion would unphysiologically reduce ^{18}F-PET RBC signal in healthy brain tissue (bearing normal, unimpeded circulation). This would inaccurately over-represent ^{18}F-PET RBC signal at the site of hemorrhage (where RBC circulation is expected to be more stagnant). **Asymmetric intracranial hemorrhage in ^{18}F- RBC PET scans is visible in all bearing brain specimens. PET data is corroborated by bright field imaging in all specimens.**

Supporting figure 13a. (Figure 3a and 4a) Injection 10 min before lesion

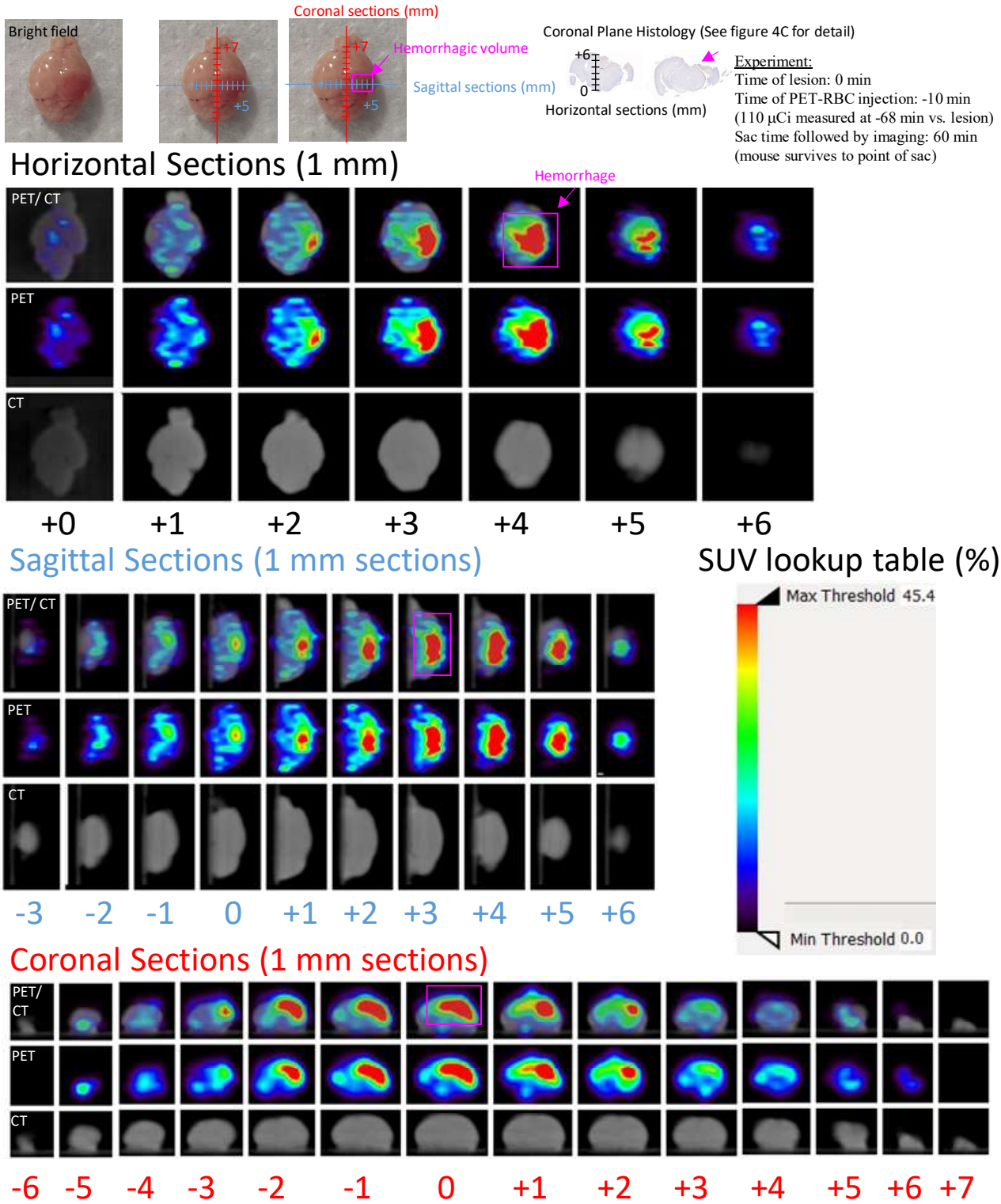

Supporting figure 13b. (Supporting Figure 5A) Injection 5 min before lesion

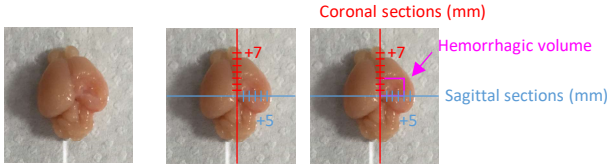

Experiment:
Time of lesion: 0 min
Time of PET-RBC injection: -5 min
(14 µCi measured at -19 min vs. lesion)
Sac time followed by brain imaging: 60 min
(mouse survives to point of sac)

Horizontal Sections (1 mm) – Note: all sections to scale

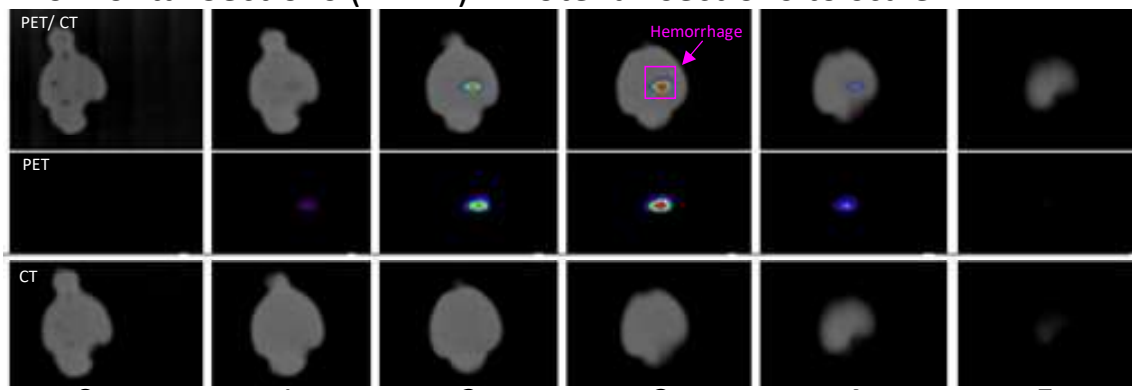

+0 +1 +2 +3 +4 +5 (mm from base)

Sagittal Sections (1 mm sections)

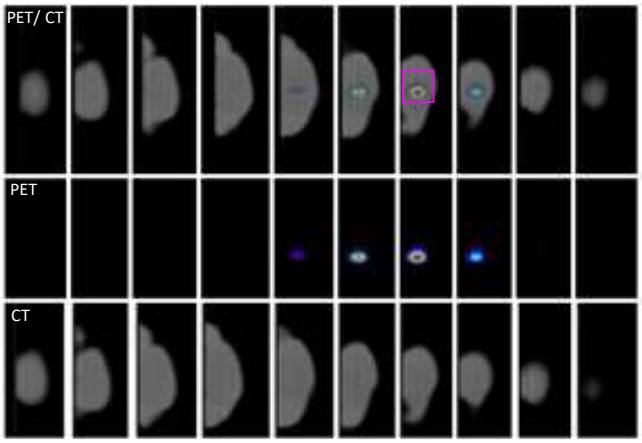

-4 -3 -2 -1 0 +1 +2 +3 +4 +5

SUV lookup table (%)

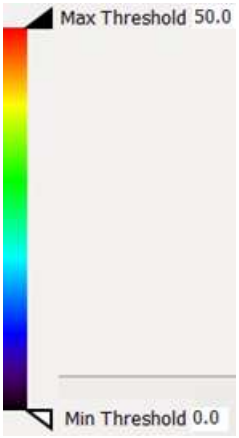

Coronal Sections (1 mm sections)

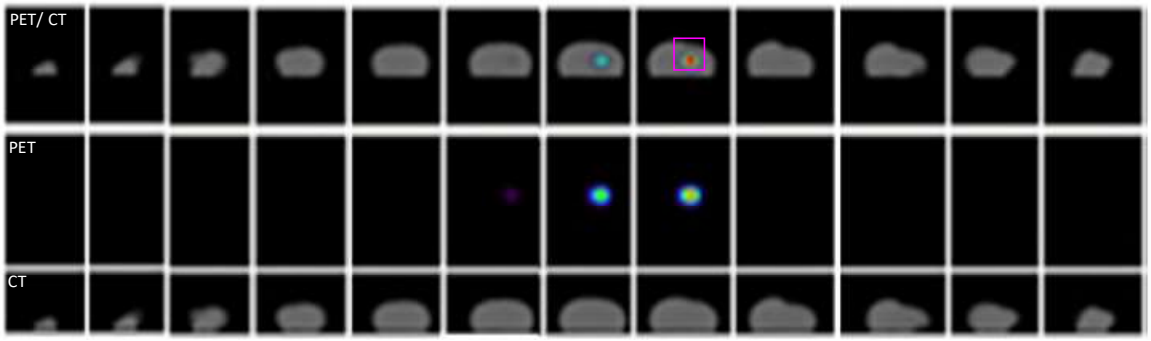

-5 -4 -3 -2 -1 0 +1 +2 +3 +4 +5 +6

Supporting figure 13*c*. *(Supporting Figure 6Aiii)* Injection 11 min after lesion

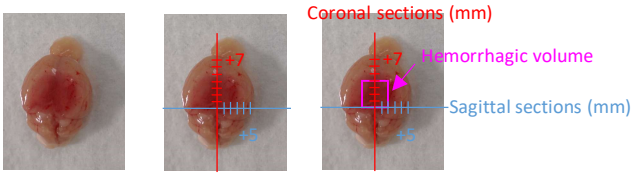

Experiment:
Time of lesion: 0 min
Time of PET-RBC injection: +11 min
(39.6 µCi measured at -+41 min vs. lesion)
Time of death: +35 min
(Mouse dies before predetermined point of sacrifice)
Time of brain imaging: 91 min

Horizontal Sections (1 mm) – Note all sections to scale

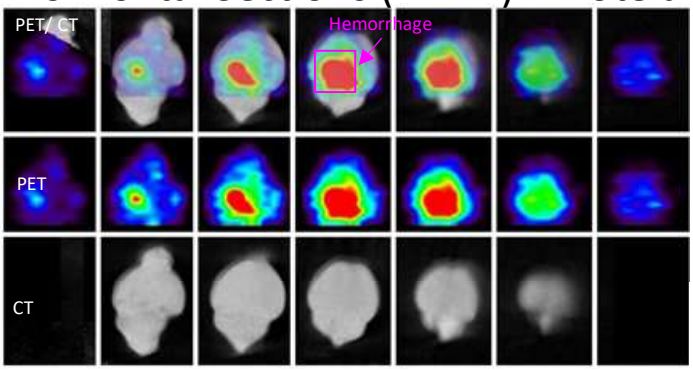

+0 +1 +2 +3 +4 +5 +6

SUV lookup table (%)

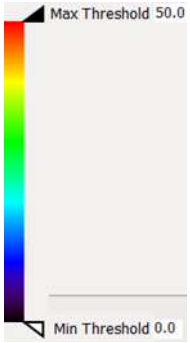

Sagittal Sections (1 mm sections)

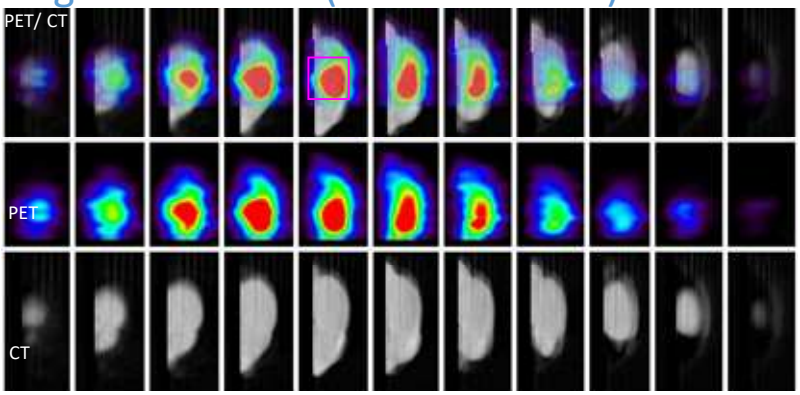

-4 -3 -2 -1 0 +1 +2 +3 +4 +5

Coronal Sections (1 mm sections)

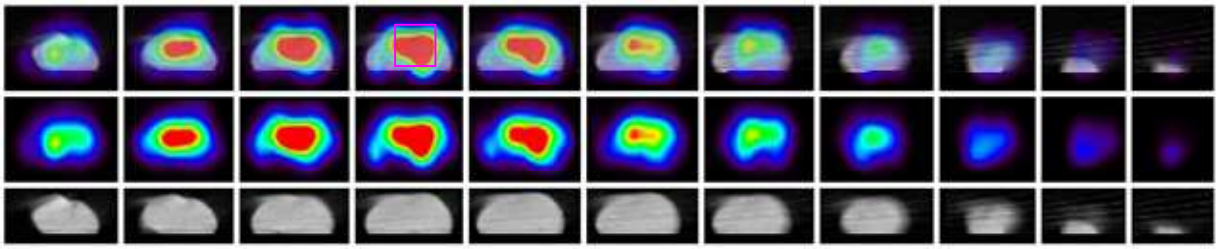

-1 0 +1 +2 +3 +4 +5 +6 +7 +8 +9

Supporting figure 13d. (Supporting Figure 6Biii) Injection 26 min after lesion

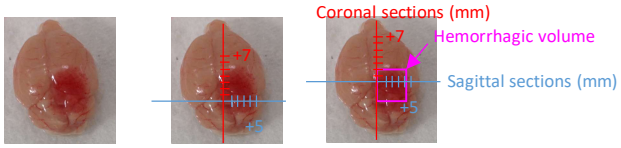

Experiment:
Time of lesion: 0 min
Time of PET-RBC injection: +26 min
(40 µCi measured at +46 min vs. lesion)
Sac time followed by brain imaging: 82 min
(mouse survives to point of sac)

Horizontal Sections (1 mm) – Note all sections to scale

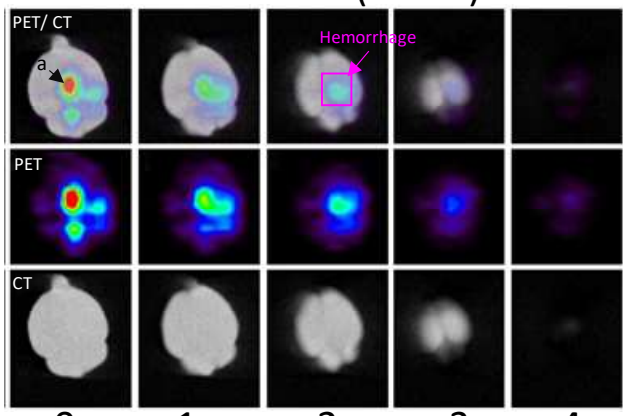

Sagittal Sections (1 mm sections)

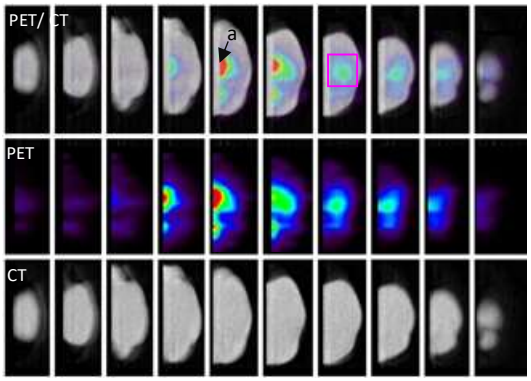

SUV lookup table (%)

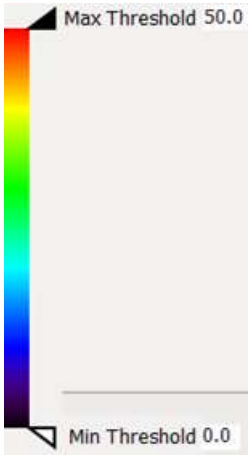

Coronal Sections (1 mm sections)

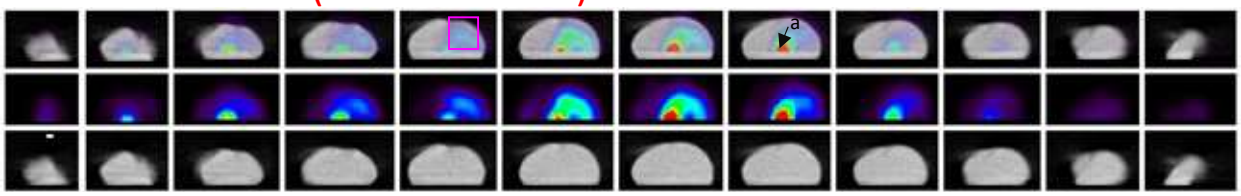

a. Blood accumulation at the base of the brain (+0/+1 mm Horizontal section) from ex vivo drainage following organ excision

Supporting figure 13d. (Supporting Figure 7Dii) Injection 47 min before lesion

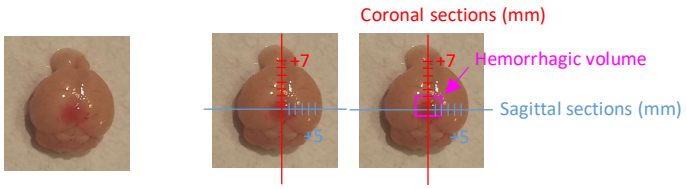

Experiment:
Time of lesion: 0 min
Time of PET-RBC injection: -47 min
(172 µCi measured at -70 min vs. lesion)
Sac time followed by brain imaging: 53 min
(mouse survives to point of sac)

Horizontal Sections (1 mm) – Note all sections to scale

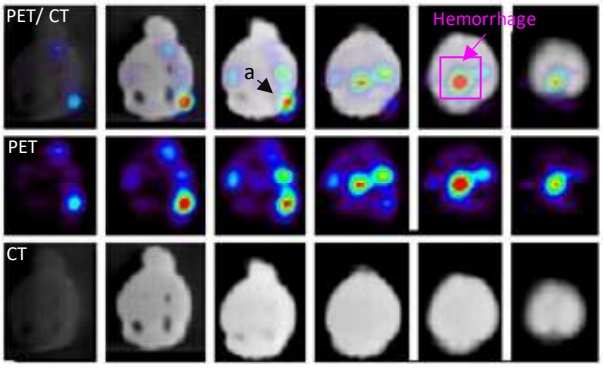

Sagittal Sections (1 mm sections)

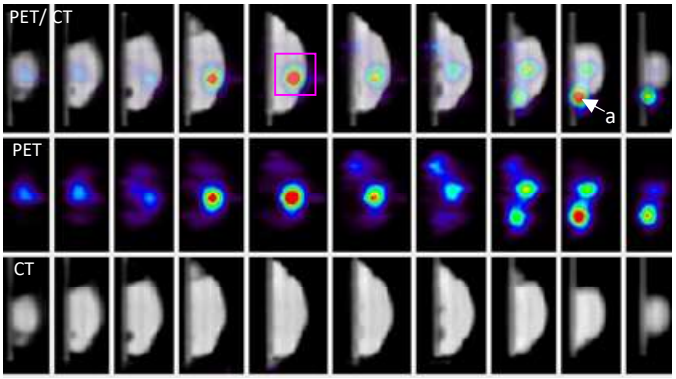

SUV lookup table (%)

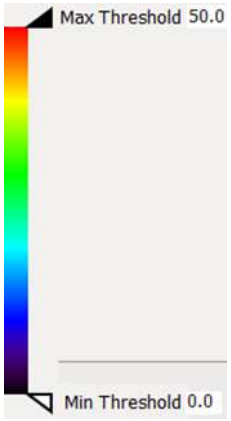

Coronal Sections (1 mm sections)

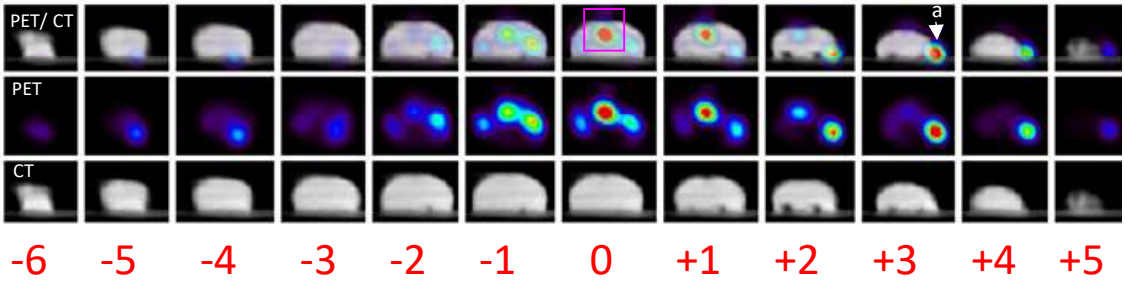

a. Bleeding unrelated to cryolesion. Exsanguination/perfusion is not performed prior to ex vivo tissue resection. Blood accumulation at the base of the brain (+0/+1 mm Horizontal section) from ex vivo drainage following organ excision

Supporting figure 13f. (Supporting Figure 9A, Cohort B, M4) Injection 5 min after lesion

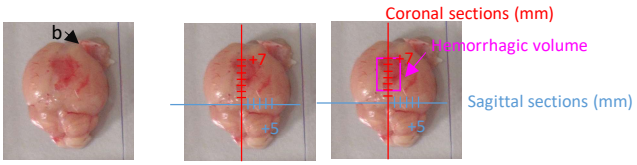

Experiment:
Time of lesion: 0 min
Time of PET-RBC injection: +5 min
(105 µCi measured at -9 min vs. lesion)
Sac time followed by brain imaging: 181 min
(mouse survives to point of sac)

Horizontal Sections (1 mm) – Note all sections to scale

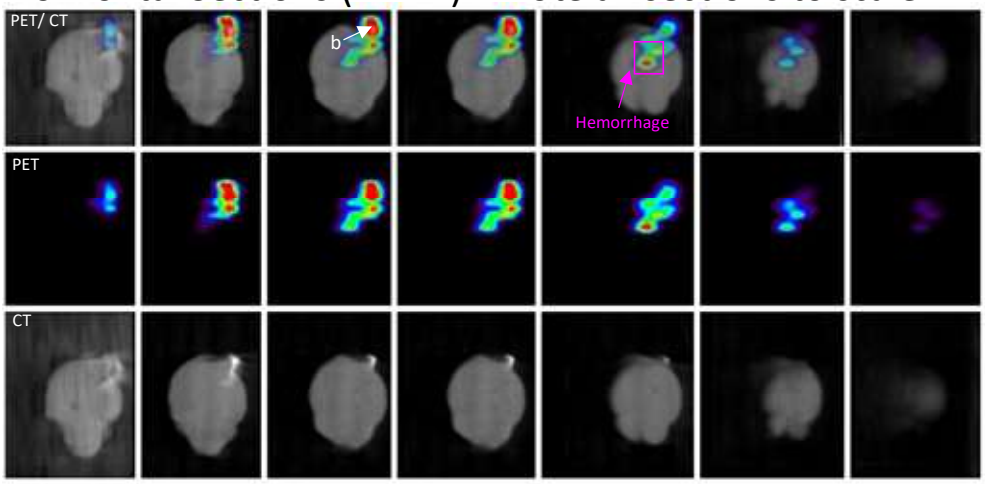

+0 +1 +2 +3 +4 +5 +6

Sagittal Sections (1 mm sections)

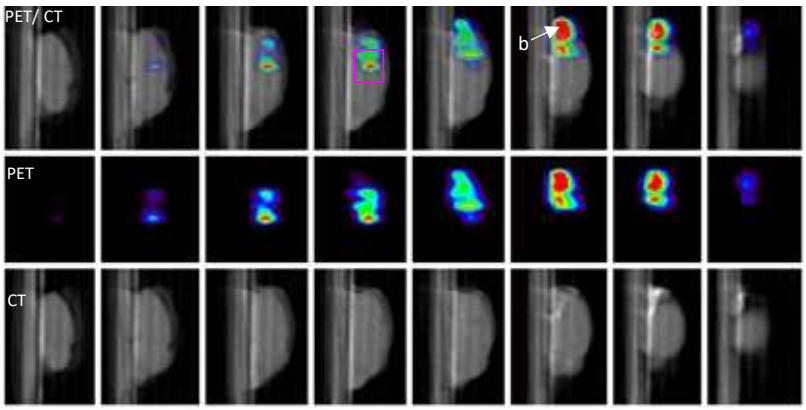

-2 -1 0 +1 +2 +3 +4 +5

SUV lookup table (%)

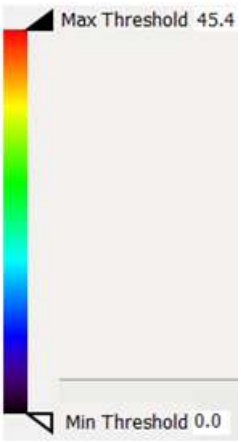

Coronal Sections (1 mm sections)

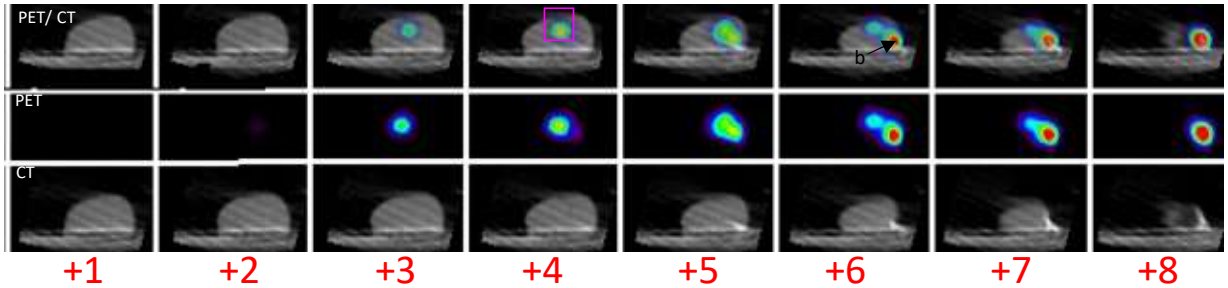

+1 +2 +3 +4 +5 +6 +7 +8

b. Bleeding in olfactory bulb (observable in bright field image)

Supporting figure 13g. (Supporting Figure 9A, Cohort B, M6) Injection 5 min after lesion

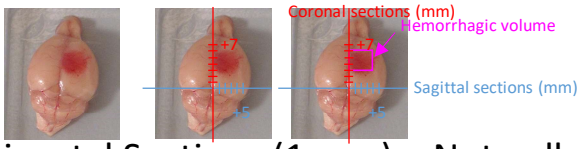

Experiment:
Time of lesion: 0 min
Time of PET-RBC injection: +5 min
(105 µCi measured at -21 min vs. lesion)
Sac time followed by brain imaging: 169 min
(mouse survives to point of sac)

Horizontal Sections (1 mm) – Note all sections to scale

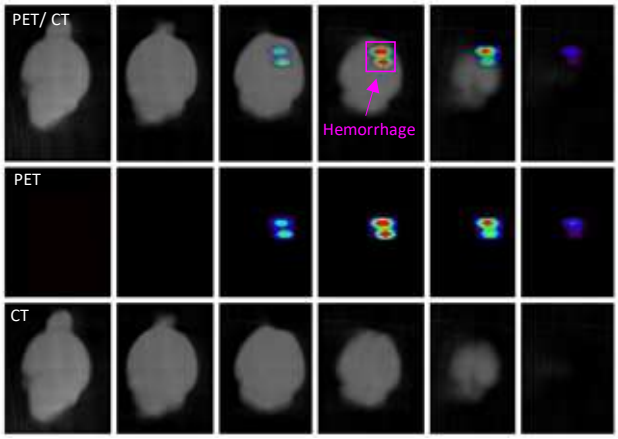

+0 +1 +2 +3 +4 +5

Sagittal Sections (1 mm sections)

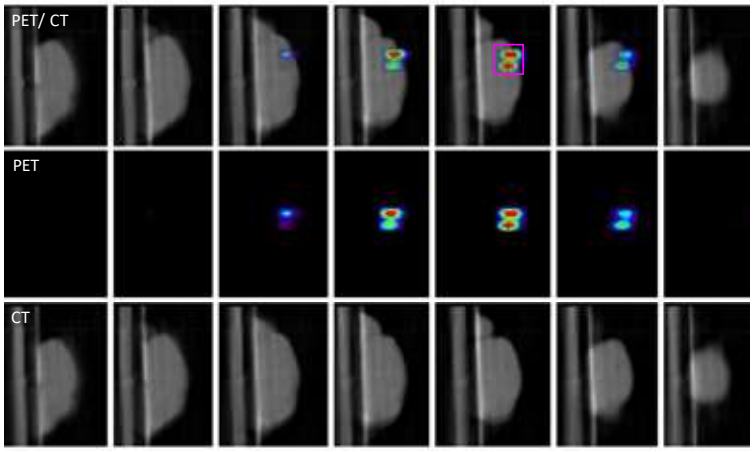

-1 0 +1 +2 +3 +4 +5

SUV lookup table (%)

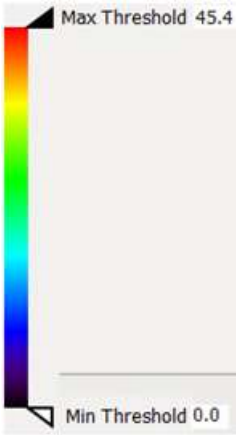

Coronal Sections (1 mm sections)

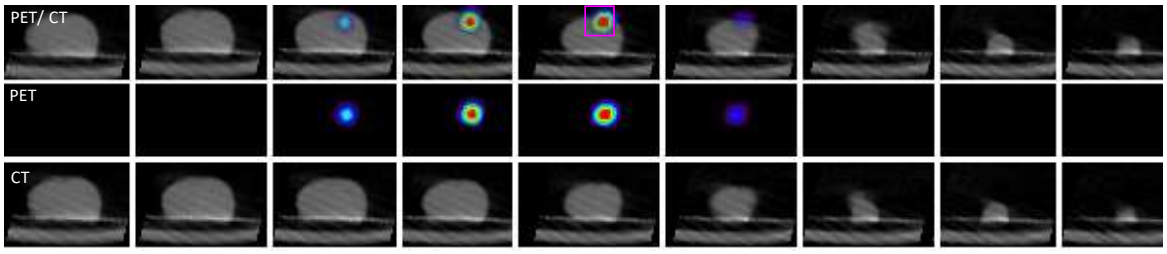

+1 +2 +3 +4 +5 +6 +7 +8 +9

Supporting figure 13h. (Supporting Figure 11A) Injection 107 min after lesion

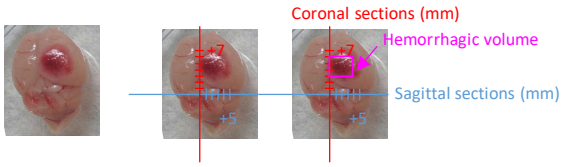

Experiment:
Time of lesion: 0 min
Time of PET-RBC injection: +107 min
(78 µCi measured at -19 min vs. lesion)
Sac time followed by brain imaging: 195 min
(mouse survives to point of sac)

Horizontal Sections (1 mm) – Note all sections to scale

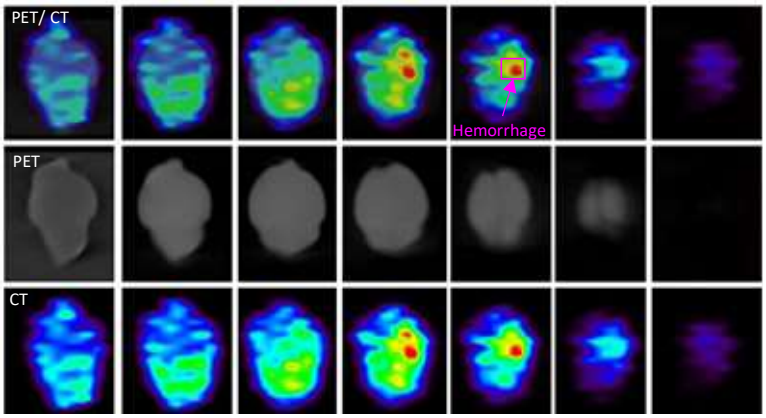

+0 +1 +2 +3 +4 +5 +6

SUV lookup table (%)

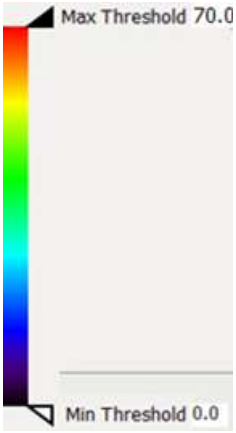

Sagittal Sections (1 mm sections)

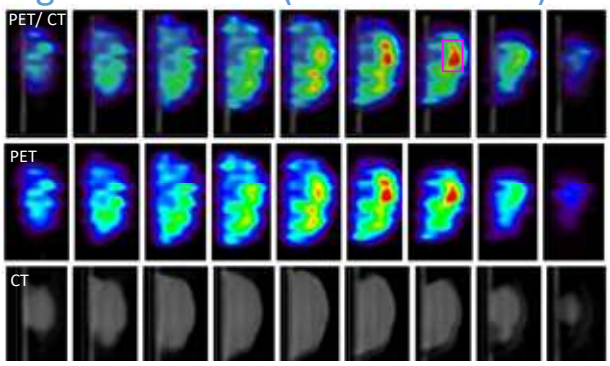

-4 -3 -2 -1 0 +1 +2 +3 +4

Coronal Sections (1 mm sections)

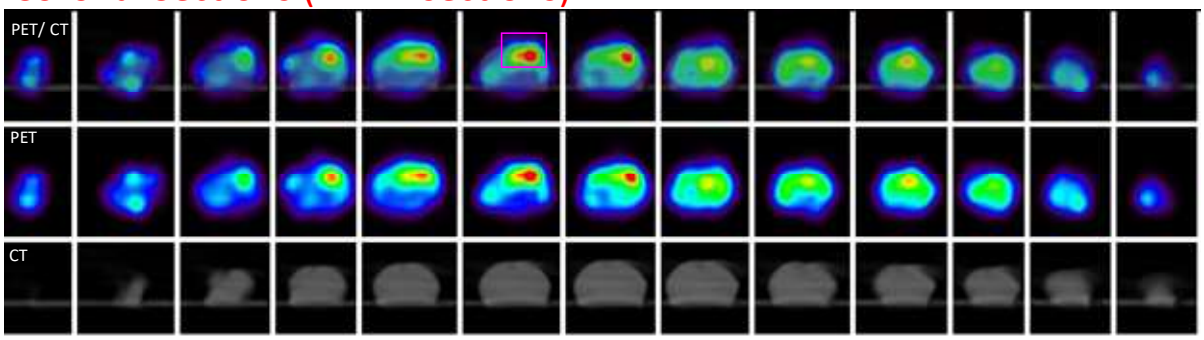

0 +1 +2 +3 +4 +5 +6 +7 +8 +9 +10 +11 +12

Supporting figure 13i.(Supporting Figure 11B) Injection 95 min after lesion

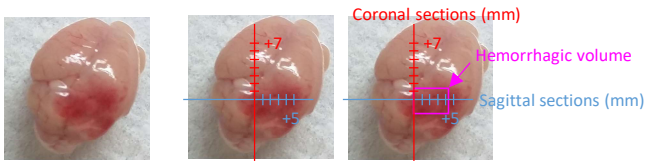

Experiment:
Time of lesion: 0 min
Time of PET-RBC injection: +95 min
(78 µCi measured at -29 min vs. lesion)
Sac time followed by brain imaging: 182 min
(mouse survives to point of sac)

Horizontal Sections (1 mm)

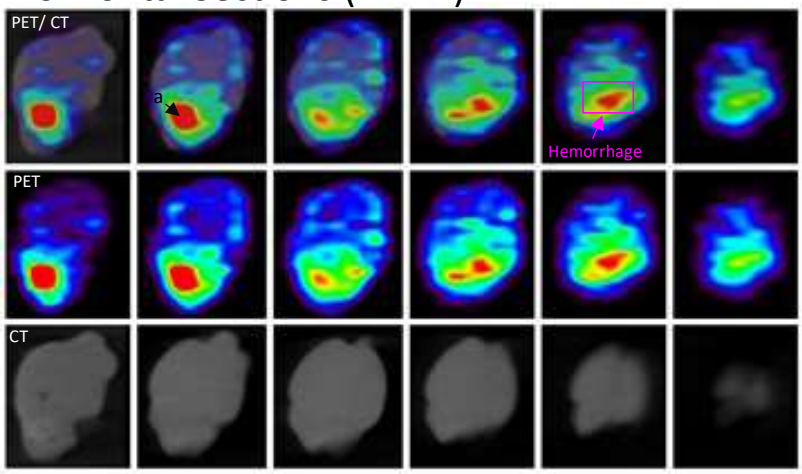

SUV lookup table (%)

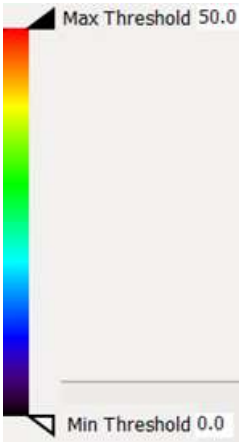

Sagittal Sections (1 mm sections)

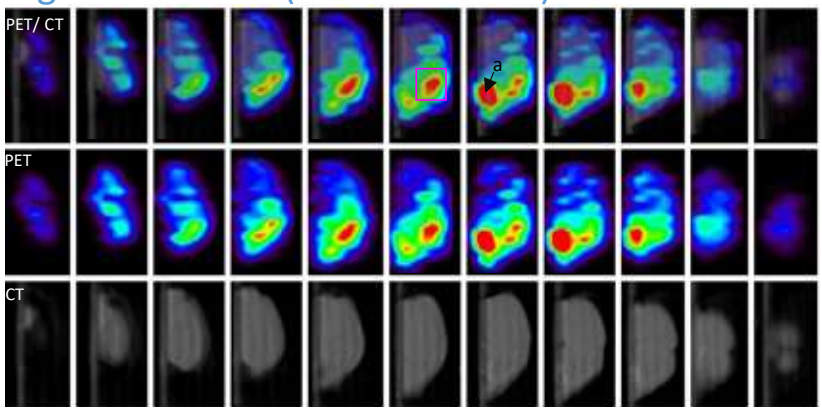

Coronal Sections (1 mm sections)

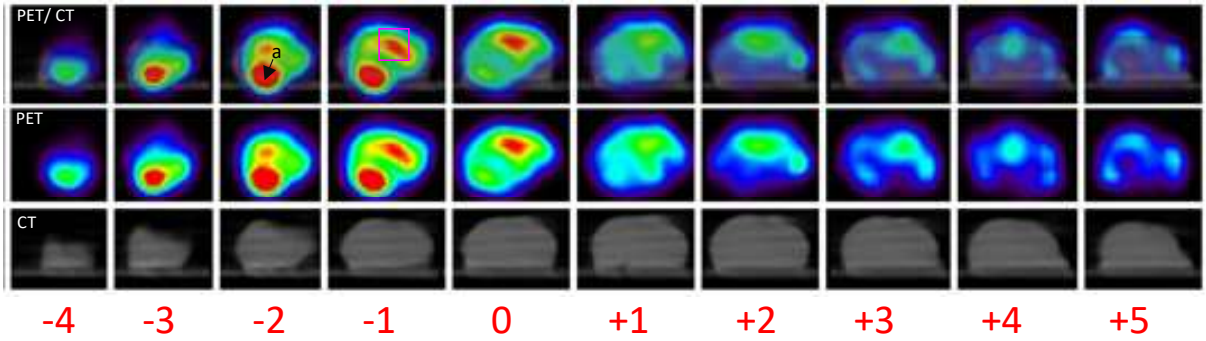

a. Blood accumulation at the base of the brain (+0/+1 mm Horizontal section) from ex vivo drainage following organ excision

Supporting figure 13j.(Supporting Figure 11C) Injection 30 min after lesion

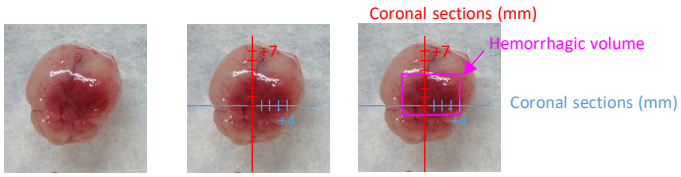

Horizontal Sections (1 mm)

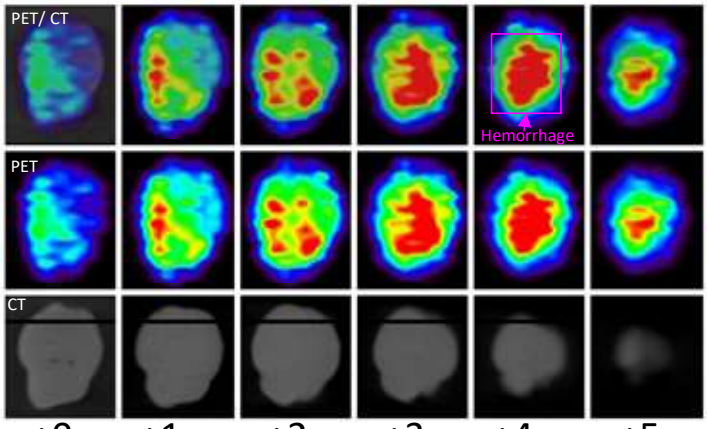

+0 +1 +2 +3 +4 +5

Experiment:
Time of lesion: 0 min
Time of PET-RBC injection: +30 min
(78 µCi measured at -106 min vs. lesion)
Time of death: +61 min
(Mouse dies before predetermined point of sacrifice)
Time of brain imaging: 118 min

Sagittal Sections (1 mm sections)

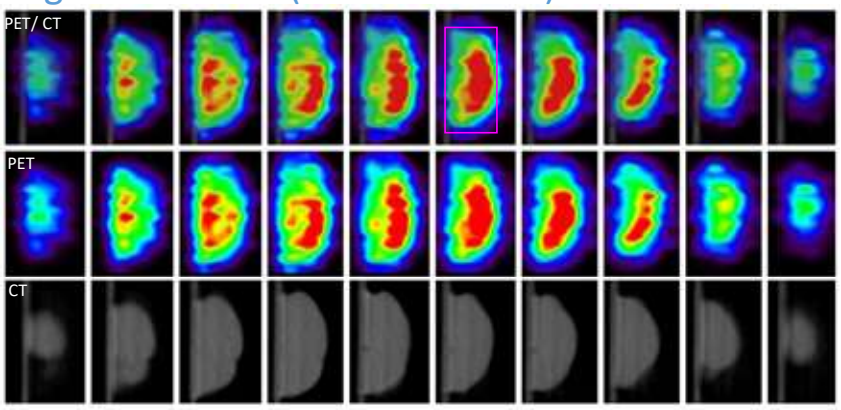

-4 -3 -2 -1 0 +1 +2 +3 +4 +5

SUV lookup table (%)

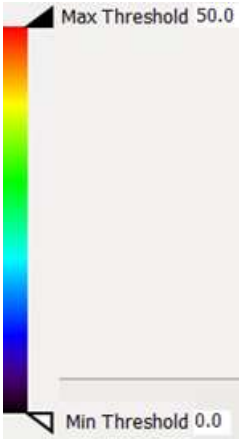

Transverse Sections (1 mm sections)

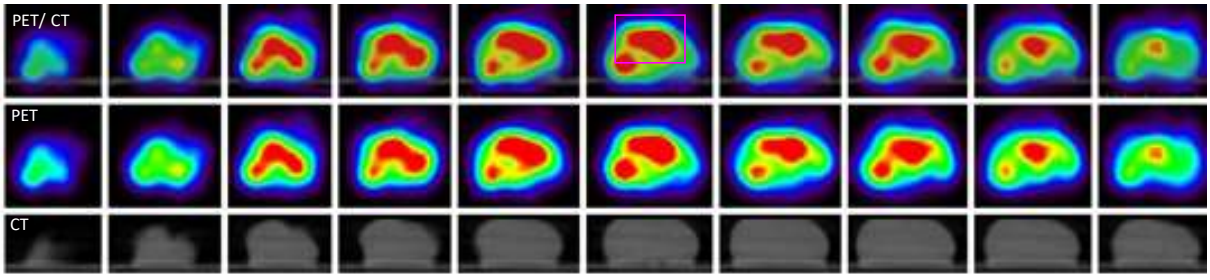

-4 -3 -2 -1 0 +1 +2 +3 +4 +5

Supporting figure 13k.(Supporting Figure 11D) Injection 14 min after lesion

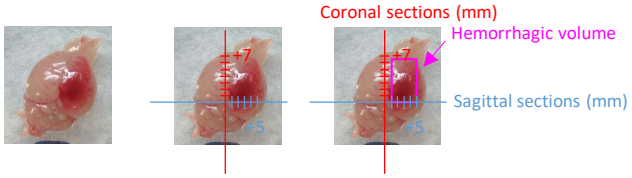

Experiment:
Time of lesion: 0 min
Time of PET-RBC injection: +14 min
(78 µCi measured at -118 min vs. lesion)
Sac time followed by brain imaging: 102 min
(mouse survives to point of sac)

Horizontal Sections (1 mm)

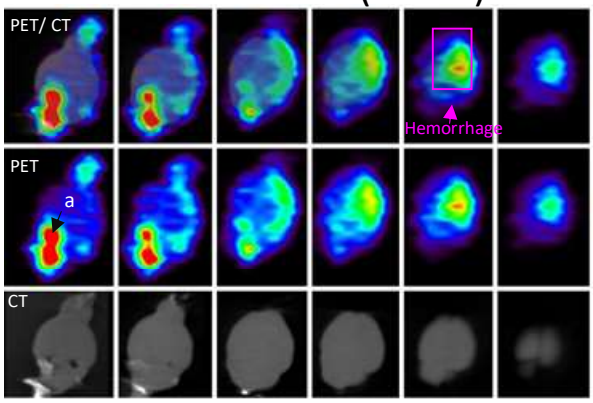

+0 +1 +2 +3 +4 +5

Sagittal Sections (1 mm sections)

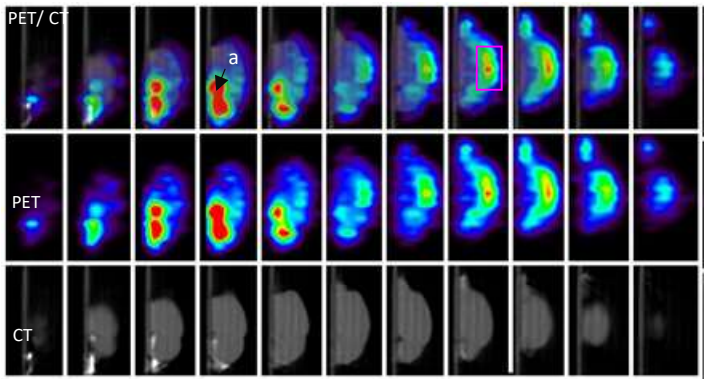

-4 -3 -2 -1 0 +1 +2 +3 +4 +5 +6

SUV lookup table (%)

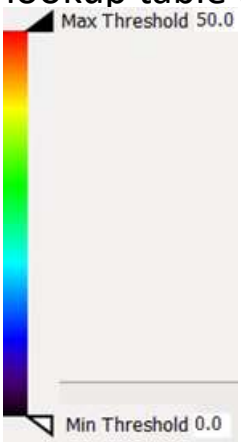

Coronal Sections (1 mm sections)

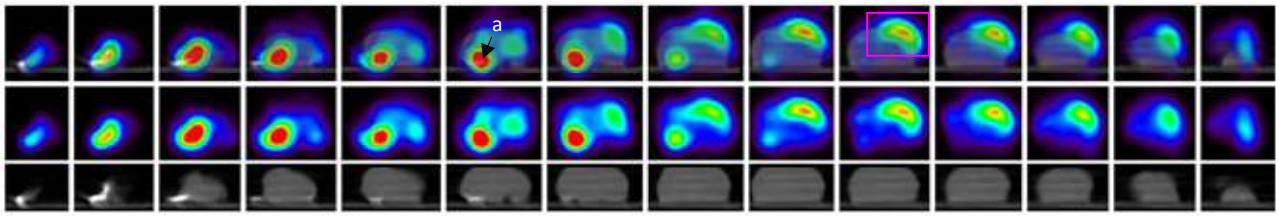

-5 -4 -3 -2 -1 0 +1 +2 +3 +4 +5 +6 +7 +8

a. Blood accumulation at the base of the brain (+0/+1 mm Coronal section) from ex vivo drainage following organ excision

Supporting figure 13I.(Supporting Figure 11E) Injection 12 min after lesion

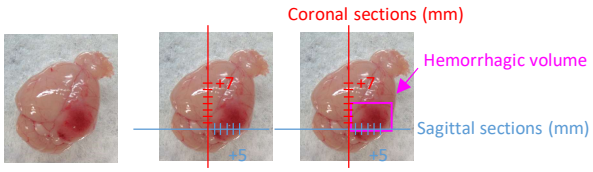

Experiment:
Time of lesion: 0 min
Time of PET-RBC injection: +12 min
(78 µCi measured at -118 min vs. lesion)
Sac time followed by brain imaging: +100 min
(mouse survives to point of sac)

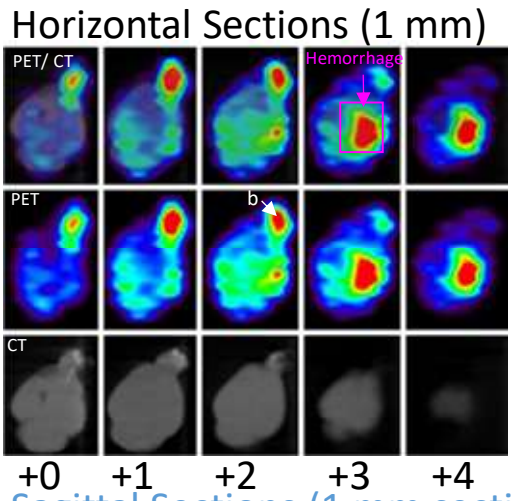

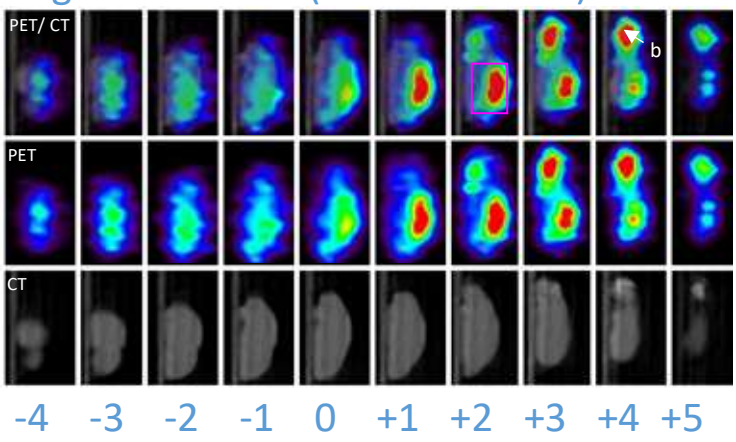

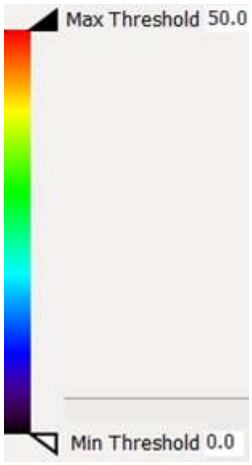

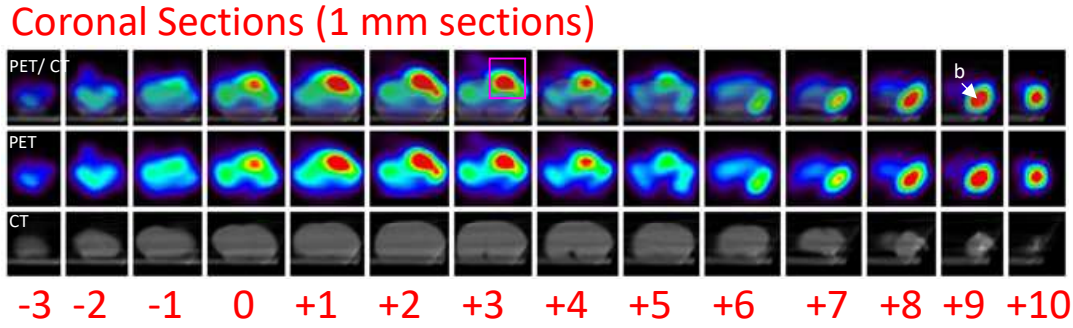

b. Bleeding in olfactory bulb

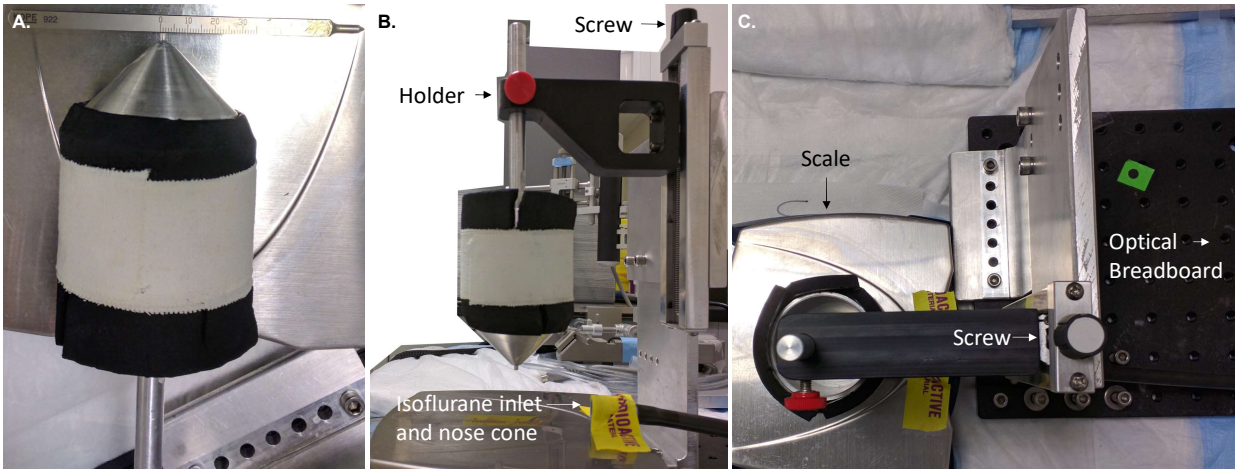

Supporting figure 14. Preferred surgical setup. (**A**) Machined cryolesion cylinder modified from Raslan, F, et. al. Focal brain trauma in the cryogenic lesion model in mice. Experimental & Translational Stroke Medicine, 2012, 4:6. DOI: 10.1186/2040-7378-4-6. The cryoprobe has been altered so that the tip diameter is 2.0 mm and is machined from aluminum instead of copper. (**B**) The apparatus is secured in a holder via a screw that allows a user to raise or lower the cryoprobe to adjust contact time and force over the cryolesion focal point. The specimen is secured in an isoflurane supply on a scale in an area that is well vented for isoflurane work. (**C**) Overhead view of the setup in (**B**) showing the positioning of the cryoprobe fixed on an optical breadboard. Ideally, a stereotaxic frame ((**B**) background) should be placed on top of the tared scale and mice fixed in position by ear bars.

Synthetic Chemistry:

Supporting figure 15. tri- and penta-methane N-hydroxy succinimide bearing boronate/fluorescent probe synthesis (**1**), (**2**)

The synthesis of the PET/NIRF agent, **1** and **2**, was done in a single, two step reaction (scheme S1). The final yield of **1** was 30%. The final yield of **2** was 15%.

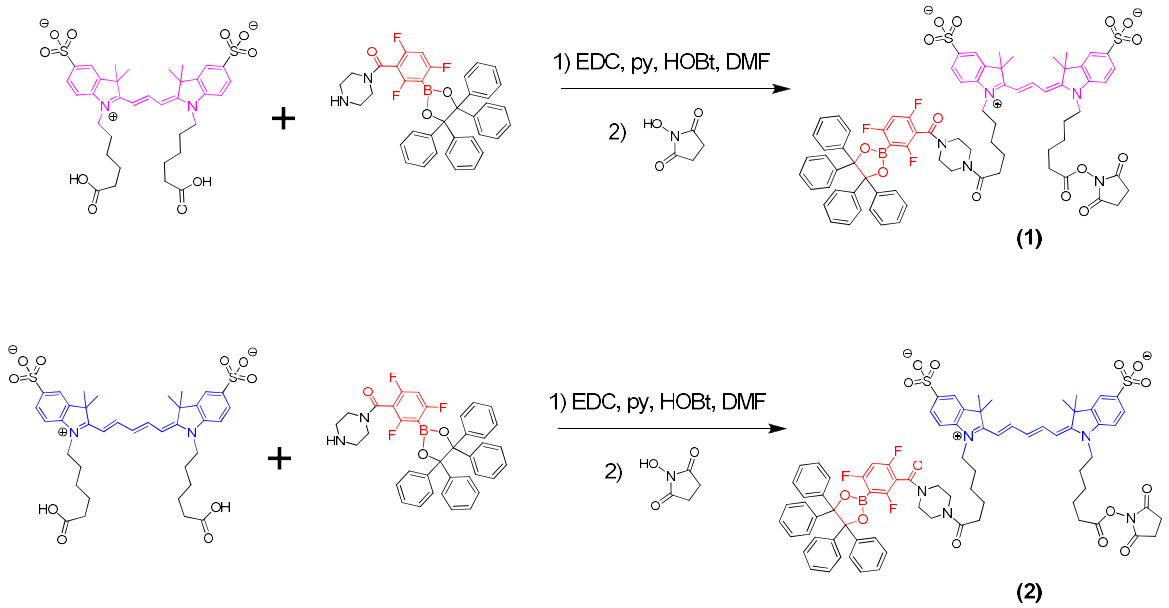

Supporting figure 15. Scheme S1. Synthesis of NHS ester bearing boronated, [18/19F]-PET/NIRF precursors, 1, modified with a biotin. The boron based fluoride trap is shown in orange, the Cy3 NIR fluorophore is shown in magenta, and the Cy5 NIR fluorophore is shown in blue.

General synthetic methods

Chemicals were purchased from Oakwood Chemical, Aldrich, Combi-blocks, Strem, and Alfa Aesar. CY3.18.OH and CY5.18.OH fluorophores were synthesized according to literature (Ref. 28). CY3.18.OH and CY5.18.OH were also commercially available. Analytical, reverse phase HPLC were performed on a Waters Acquity H class HPLC/ SQD2 mass spectrometer and a Phenomenex Kinetex 1.7µm C18 100Å, 50 cm x 2.1 mm I.D. column (00B-4475-AN), with a 1.5 min, a10-90% H_2O:acetonitrile (ACN) (0.05% TFA) gradient and a flow rate of 0.6 mL/min (unless stated otherwise). Preparative HPLC was performed on a Agilent 1200 Series HPLC equipped on a Phenomenex Luna C18(2) 100Å, 250 cm x 21.20 mm I.D. 10 µm reverse phase column (00G-4253-P0 AX), with a 20 min, a10-90% H_2O:ACN (0.05% TFA) gradient and a flow rate of 15 mL/min. ^{1}H-NMR were performed on a 500 MHz Bruker spectrometer.

Supporting figure 16. **Synthesis of dioxaborolane bearing trimethyine cyanine modified NHS ester (1)**

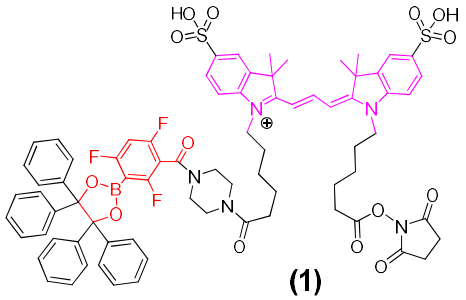

The following reagents were added to a 1.3 mL glass v-vial (Agilent #5184-3550) in the following order: CY3.18.OH (12 mg, 17 µmols, (Ref. 28)), Piperazin-1-yl(2,4,6-trifluoro-3-(4,4,5,5-tetraphenyl-1,3,2-dioxaborolan-2-yl)phenyl)methanone (12 mg, 19 µmols, (Ref. 31)), hydroxybenzotriazole monohydrate (HOBt, 14 mg, 91 µmols), 800 µL dimethylformamide (DMF), 80 µL pyridine, and N-(3-dimethylaminopropyl)-N'-ethylcarbodiimide hydrochloride (EDC, 150 mg, 785 µmols). The reaction proceeded for 2.5 hours at room temperature before an excess of N-hydroxy succinimide (15 mg, 130 µmols) was added. The reaction was left overnight at room temperature before it was chromatographed by preparative, reverse phase HPLC. Fractions containing **1** were lyophilized to give **1** (7.2 mg, 5.1 µmols, pink solid). The resulting solid was dissolved in DMSO and distributed into 1 mM 20 µL aliquots which are stored at -78°C.

UPLC-MS$^+$: a10-90%. H_2O:ACN (0.05% TFA), 1.5 min gradient, 0.6 mL/min flow, det. 1414 M/Z, 550, 280, 215 nm Abs spectra. Elution time: 1.71 min. HRMS (ESI) calculated for $C_{76}H_{76}BF_3N_5O_{14}S_2^+$ $(M)^+$: 1412.4719, found 1412.4719 (Δ 3.5 ppm).

^{1}H NMR (DMSO-d6, 500 MHz, 21 °C):

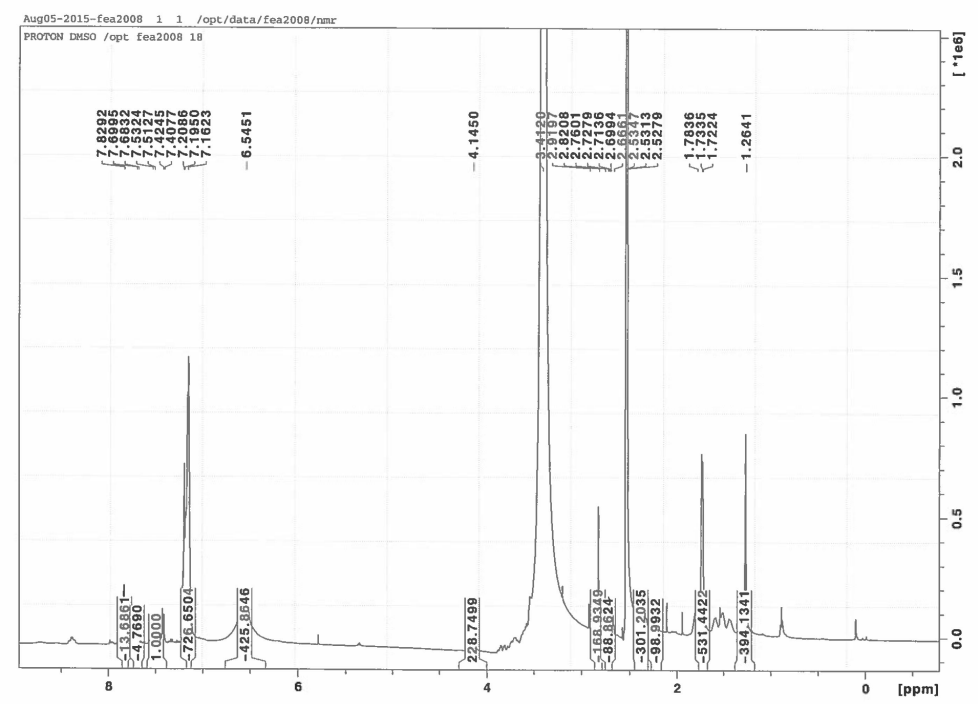

Supporting figure 16a 1H-NMR characterization of 1 in DMSO-d6.

^{13}C NMR (DMSO-d6, 500 MHz, 21 °C):

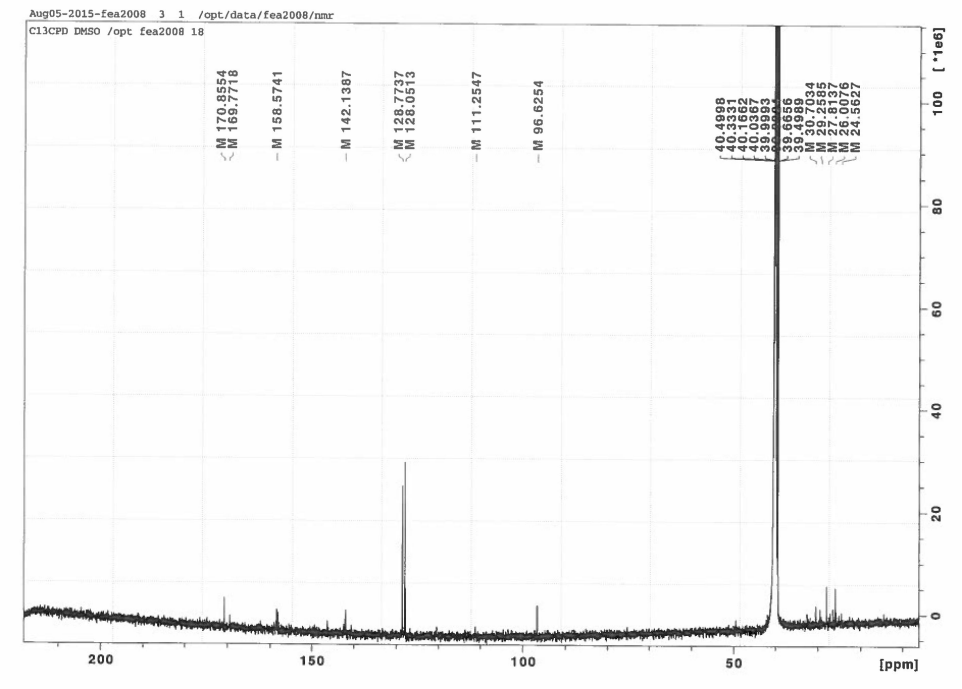

Supporting figure 16b 13C-NMR characterization of 1 in DMSO-d6.

^{19}F NMR (DMSO-d6, 500 MHz, 21 °C, TFA reference):

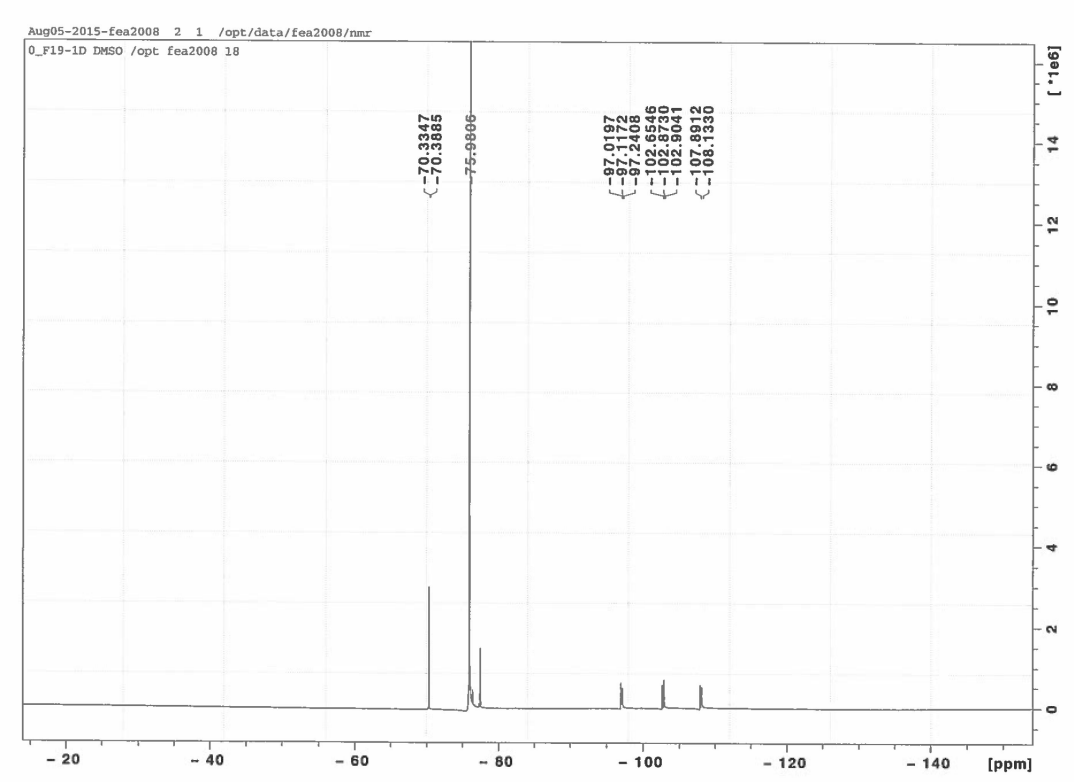

Supporting figure 16c 19F-NMR characterization of 1 in DMSO-d6.

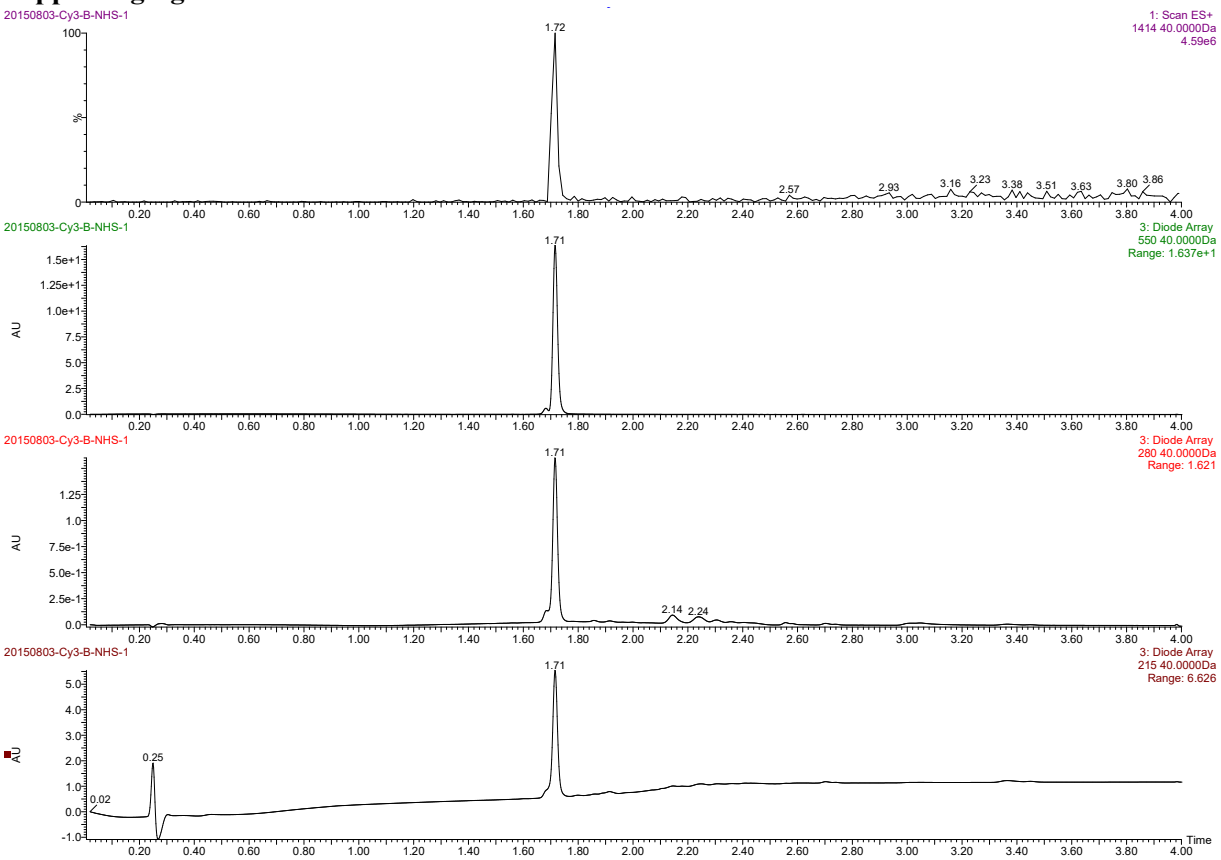

Supporting figure 16d Mass spectrometry (top 1414 MW focus) and UV vis (550 nm, 280nm and 215 nm, top to bottom traces) of 1.

Supporting figure 17. Synthesis of dioxaborolane bearing pentamethyine cyanine modified NHS ester (2)

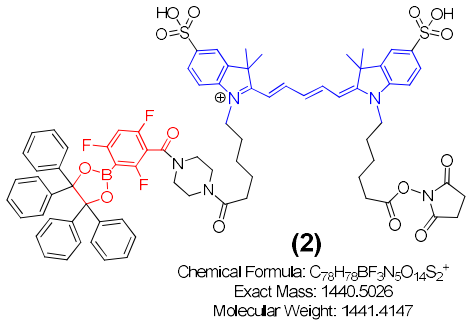

The following reagents were added to a 1.3 mL glass v-vial (Agilent #5184-3550): CY5.18.OH (12 mg, 16 µmols, (Ref. 28)), Piperazin-1-yl(2,4,6-trifluoro-3-(4,4,5,5-tetraphenyl-1,3,2-dioxaborolan-2-yl)phenyl)methanone (12 mg, 19 µmols, (Ref. 31)), HOBt (14 mg, 91 µmols), 800 µL DMF, 80 µL pyridine, and EDC (150 mg, 785 µmols). The reaction proceeded for 2.5 hours at room temperature before an excess of N-hydroxy succinimide (15 mg, 130 µmols) was added. The reaction was left overnight at room temperature before it was chromatographed by preparative, reverse phase HPLC. Fractions containing **2** were lyophilized to give **2** (3.45 mg, 2.4 µmols, blue solid). The resulting solid was dissolved in DMSO and aliquot into 1 mM 20 µL aliquots which are stored at -78°C.

UPLC-MS$^+$:a10-90% H_2O:ACN (0.05% TFA), 1.5 min gradient, 0.6 mL/min flow, det. 1441 M/Z, 215, 650, nm Abs spectra. Elution time: 1.79 min.

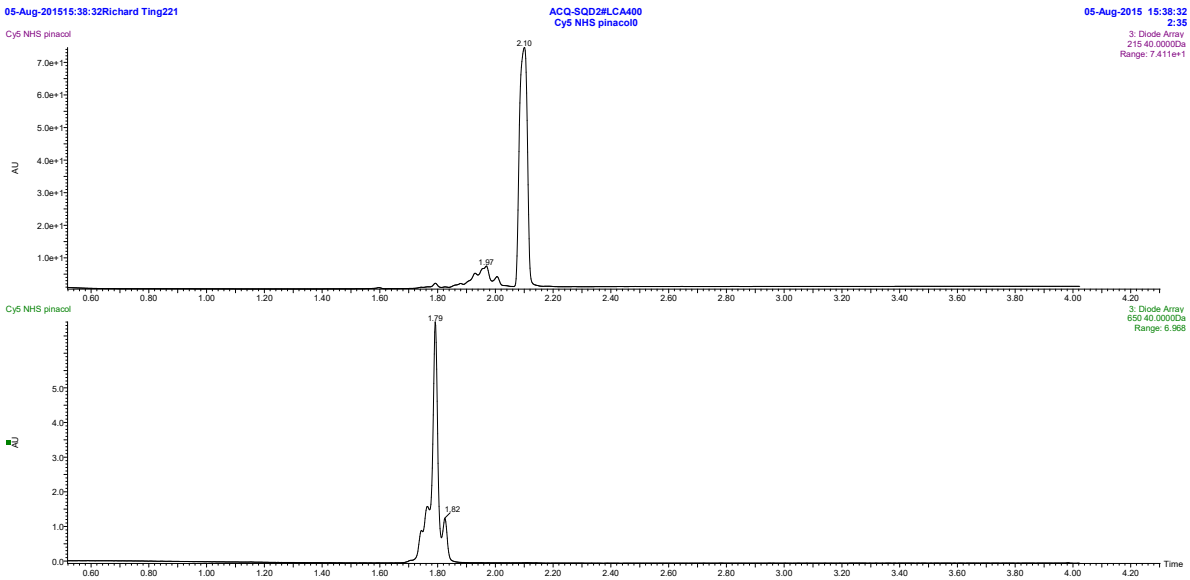

Supporting figure 17a HPLC trace of 2

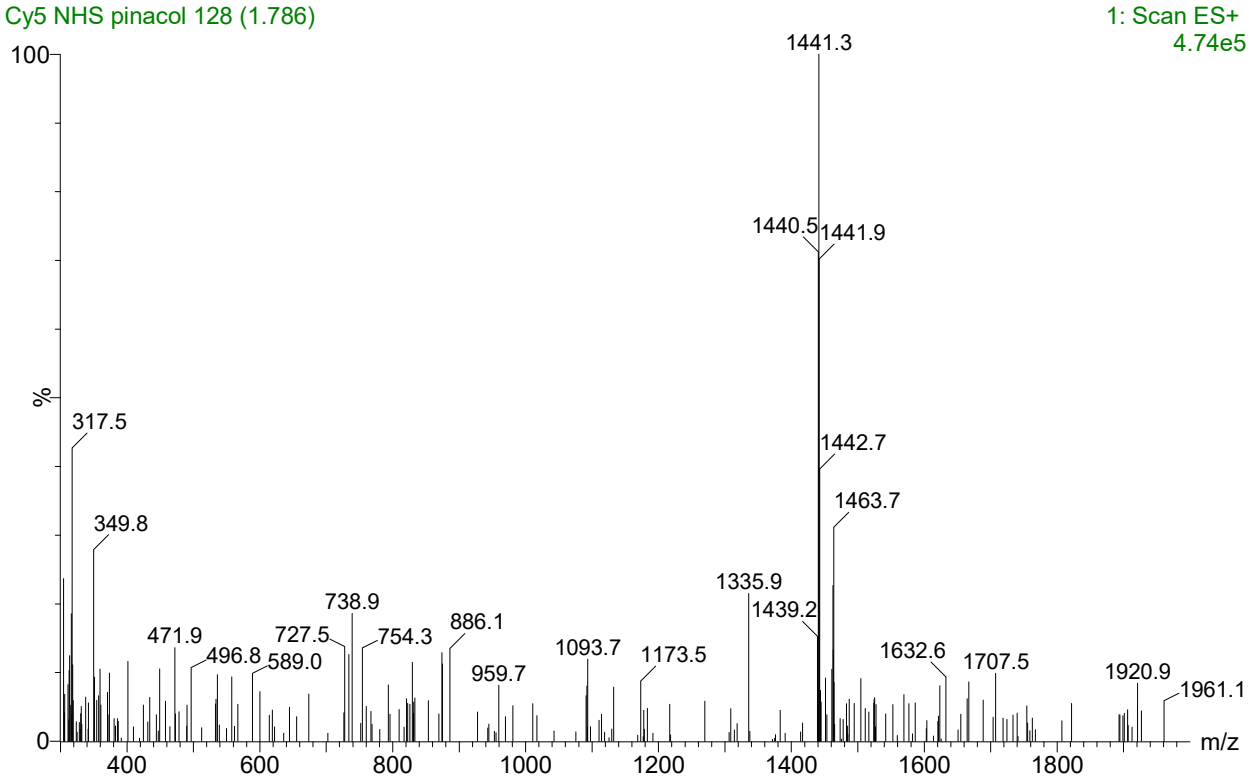

Supporting figure 17b Mass spectrometry trace of 2 at 1.786 min.

Fluoridation of NHS ester 1 and 2

Compounds **1** or **2** were reacted with 0.8 µL of 100 mM HF (80 nmols) fluoride pH 3.0, which was heated to dryness at 80˚C. Dry contents were re-suspended with a 20 µL volume of water and analyzed by reverse phase HPLC-MS.

Fluoridation of dioxaborolane bearing trimethyine cyanine modified NHS ester (1)

The fluoridation of **1** proceeds cleanly yielding only an NHS bearing fluorescent compound with absorption in the Cy3 bandwidth (550 nm).

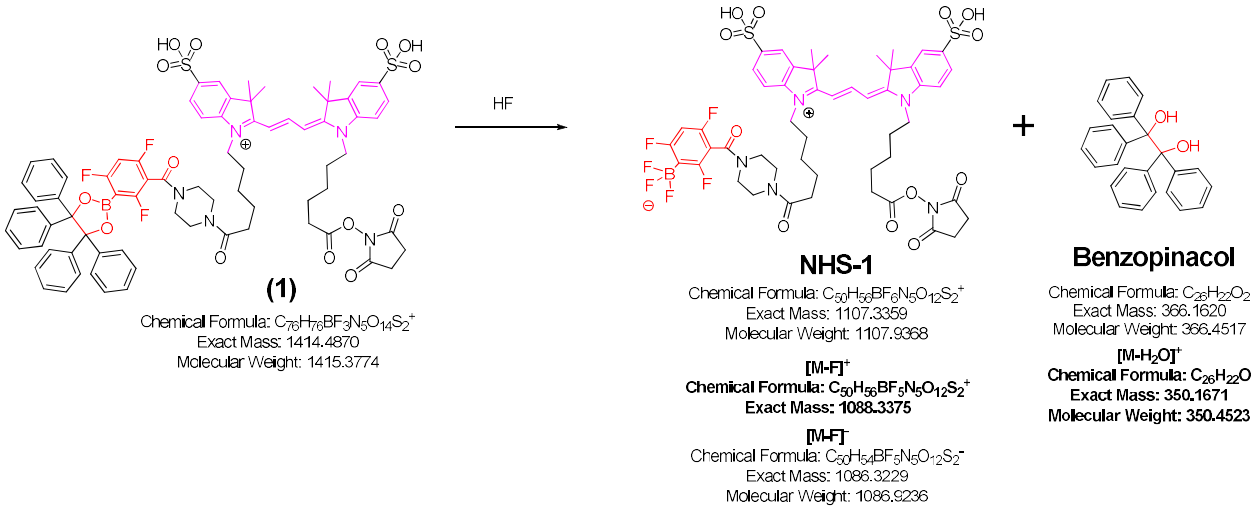

Supporting figure 18. Scheme S2. The reaction of 1 with aqueous fluoride proceeds in acidic conditions (pH 3.0) to give a trifluoroborate bearing an intact NHS ester, NHS-1 and benzopinacol

UPLC-MS$^+$ a10-90% H_2O:ACN (0.05% TFA), 1.5 min gradient, 0.6 mL/min flow, det. 1088 M/Z, 550, 215 nm Abs spectra. Elution time: 1.13 min **NHS-1**, 1.89 min pinacol. HRMS (ESI) calculated for $C_{50}H_{54}BF_5N_5O_{12}S_2^-$ $(M-F)^-$: 1086.3229, found 1086.3278 (Δ 4.5 ppm).

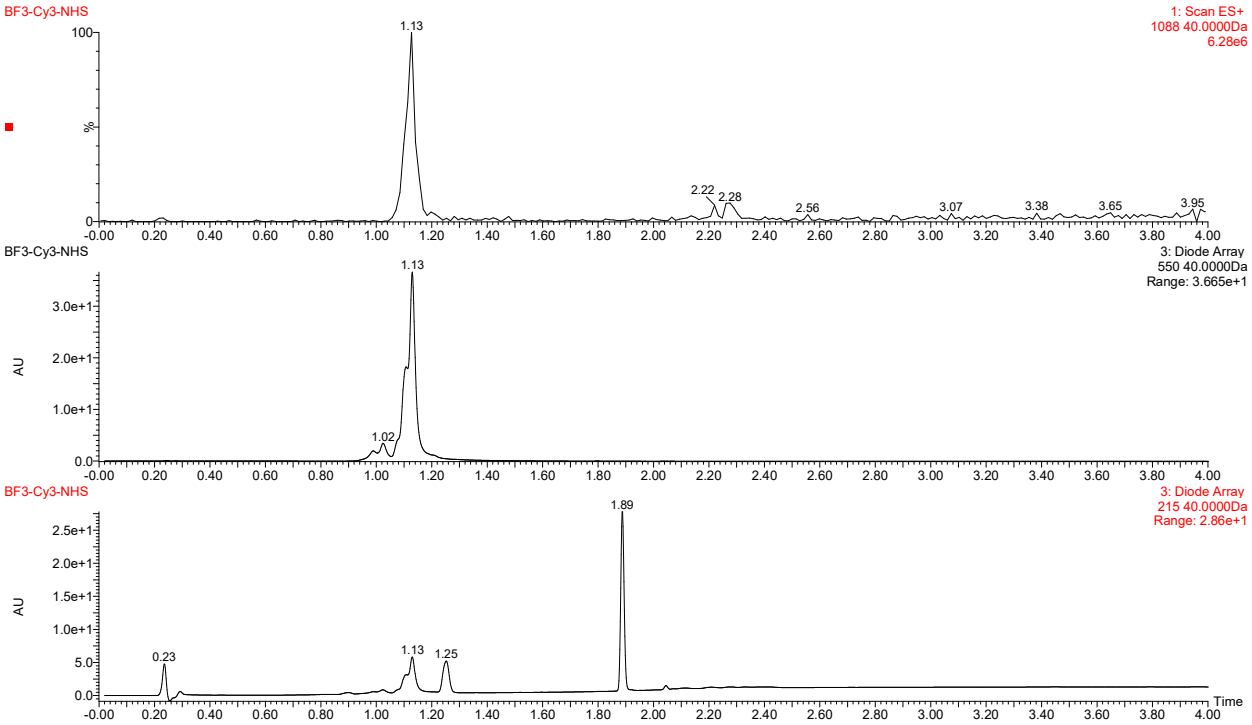

Supporting figure 18a HPLC trace of purified NHS-1

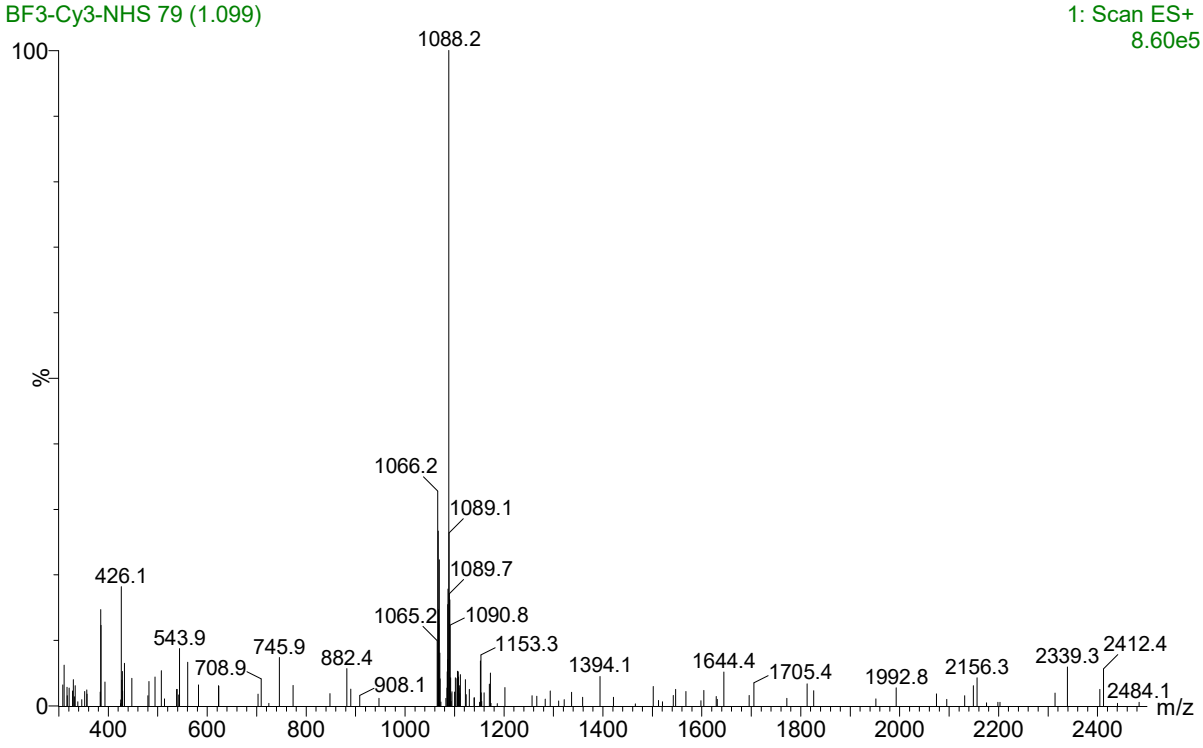

Supporting figure 18b Mass spectrometry trace of NHS-1 at 1.099 min.

^{1}H NMR (DMSO-d6, 500 MHz, 21 °C):

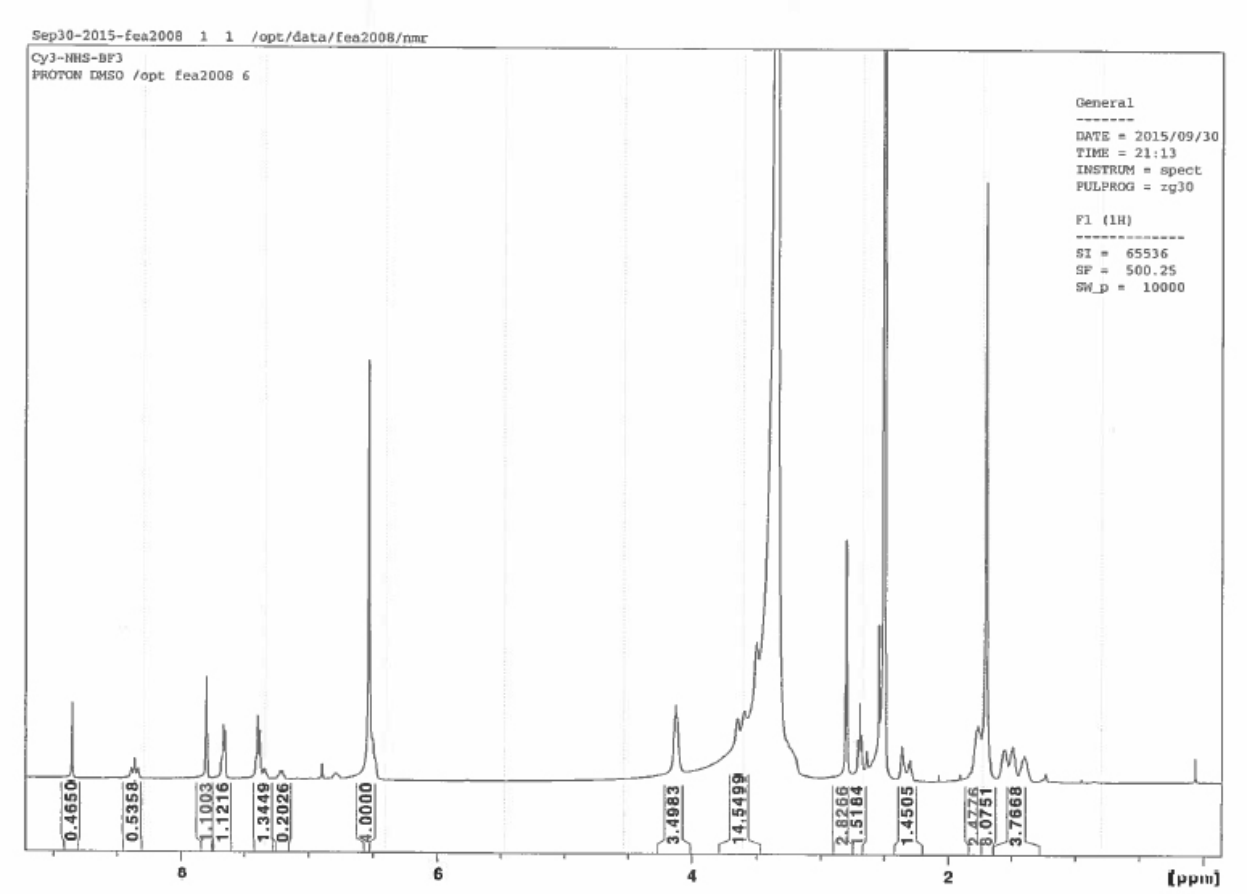

Supporting figure 18c 1H-NMR characterization of NHS-1 in DMSO-d6.

Supporting figure 19. Fluoridation of dioxaborolane bearing pentamethyine cyanine modified NHS ester (2)

The fluoridation of **2** proceeds cleanly, yielding an NHS bearing fluorescent compound with absorption in the Cy5 bandwidth (650 nm).

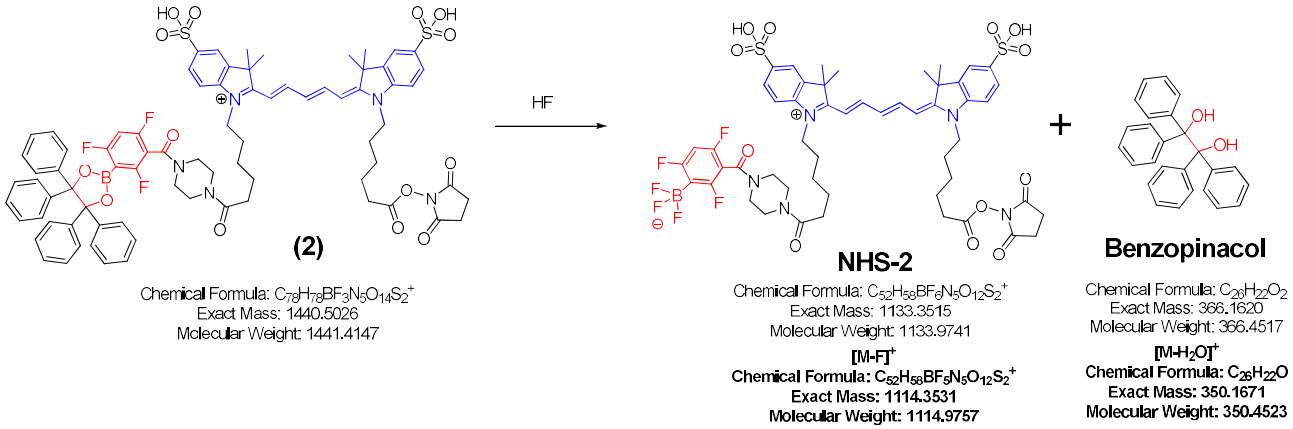

Supporting figure 19. Scheme S3. The reaction of 2 with aqueous fluoride proceeds in acidic conditions (pH 3.0) to give a trifluoroborate bearing an intact NHS ester, NHS-2, and benzopinacol

UPLC-MS$^+$:a10-90% H_2O:ACN (0.05% TFA), 1.5 min gradient, 0.6 mL/min flow, det. 1114 M/Z, 550, 215 nm Abs spectra. Elution time: 1.22 min **NHS-2**, 1.89 min pinacol.

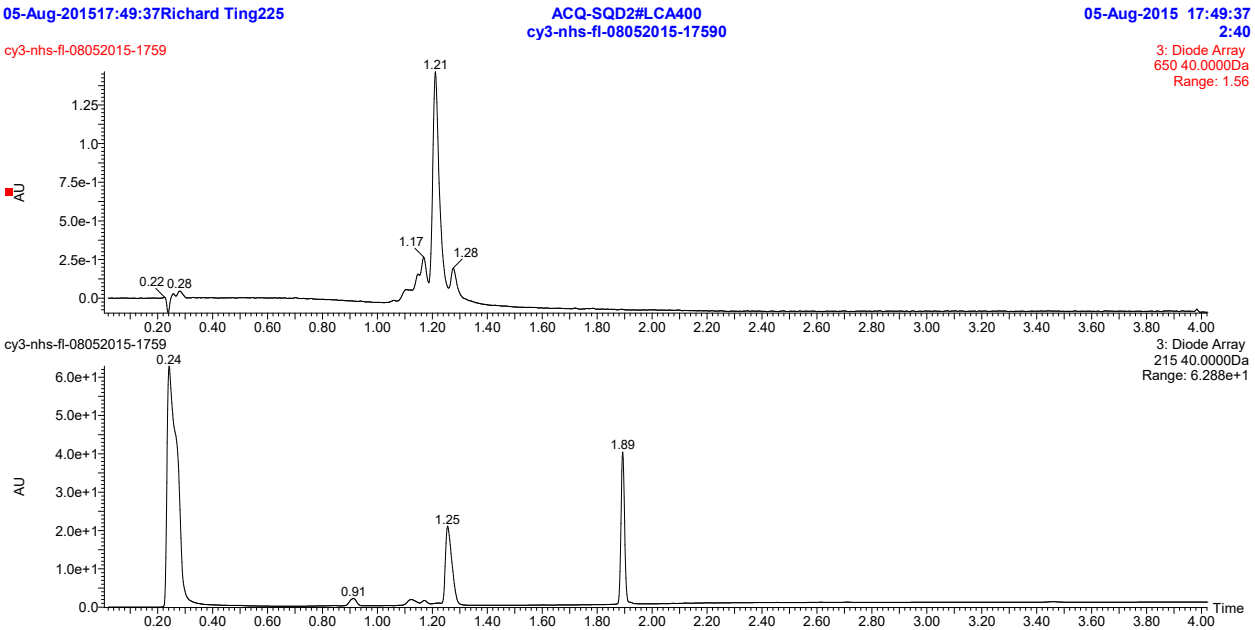

Supporting figure 19a HPLC trace of purified NHS-2

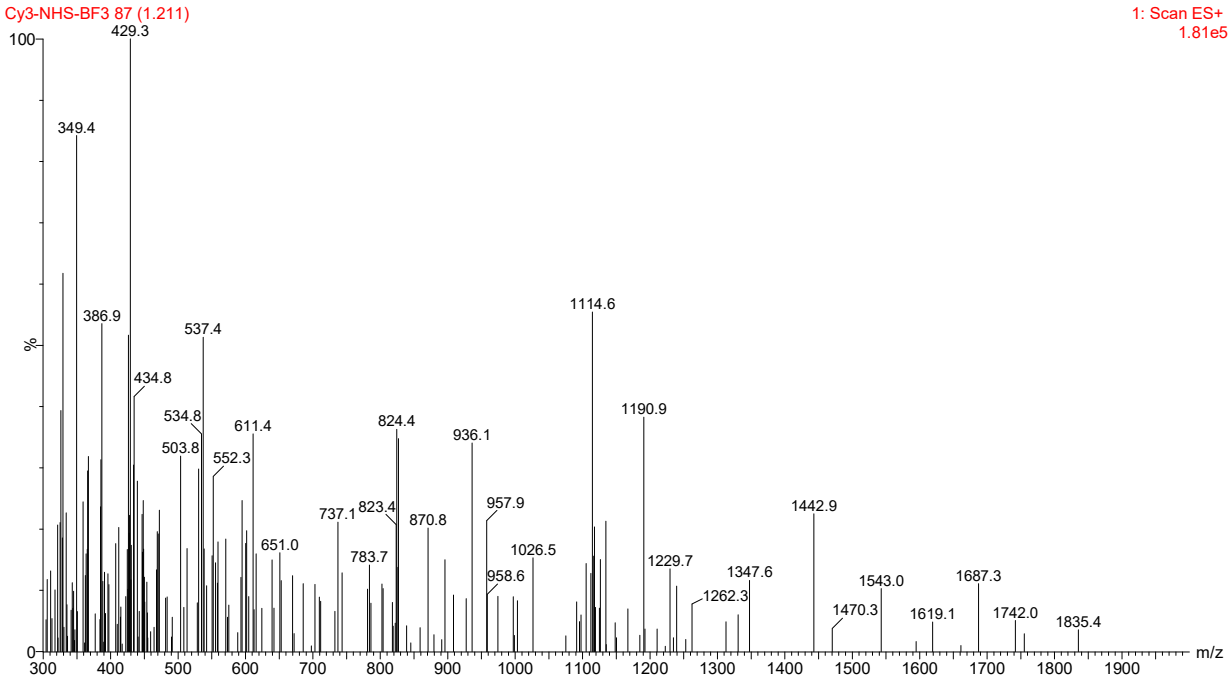

Supporting figure 19b Mass spectrometry trace of NHS-2 at 1.20 min.